OPEN ACCESS

University of BRISTOL

Link to published version (if available):
10.1029/2012JB009592

Link to publication record in Explore Bristol Research
PDF-document

University of Bristol - Explore Bristol Research

General rights

Interaction between volcanic plumes and wind during the 2010 Eyjafjallajökull eruption, Iceland

M. J. Woodhouse,[1] A. J. Hogg,[1] J. C. Phillips,[2] and R. S. J. Sparks[2]

[1]   Estimates of volcanic source mass flux, currently deduced from observations of plume height, are crucial for ash dispersion models for aviation and population hazard. This study addresses the role of the atmospheric wind in determining the height at which volcanic plumes spread in the atmosphere and the relationship between source mass flux and plume height in a wind field. We present a predictive model of volcanic plumes that describes the bending over of the plume trajectory in a crosswind and show that model predictions are in accord with a dataset of historic eruptions if the profile of atmospheric wind shear is described. The wind restricts the rise height of volcanic plumes such that obtaining equivalent rise heights for a plume in a windy environment would require an order of magnitude increase in the source mass flux over a plume in a quiescent environment. Our model calculations are used to calibrate a semi-empirical relationship between the plume height and the source mass flux that explicitly includes the atmospheric wind speed. We demonstrate that the model can account for the variations in plume height observed during the first explosive phase of the 2010 Eyjafjallajökull eruption using independently measured wind speeds and show that changes in the observed plume height are better explained by changing meteorology than abrupt changes in the source mass flux. This study shows that unless the wind is properly accounted for, estimates of the source mass flux during an explosive eruption are likely to be very significant underpredictions of the volcanic source conditions.

1.   Introduction

[2]   A major hazard arising from explosive volcanic eruptions is the injection of volcanic ash into the atmosphere and its subsequent dispersion and deposition. The largest eruptions can inject large volumes of ash at stratospheric levels which have been responsible for global temperature changes and ash deposition over thousands of square kilometers with major infrastructural and societal impacts [*Self*, 2006].

[3]   The weakly explosive phase of the 2010 eruption of Eyjafjallajökull (magnitude volcanic explosivity index [*Newhall and Self*, 1982] of 3) caused significant disruption to aviation over European airspace, highlighting the severe and extensive consequences of smaller eruptions to international infrastructure and transport. Modern commercial jet engines are susceptible to damage from low concentrations of ash, and airframes can be subject to abrasion from the suspended particulates. Prior to the 2010 Eyjafjallajökull eruption, the International Civil Aviation Organization (ICAO)

adopted a precautionary policy of ash avoidance, with no concentration of ash in the atmosphere considered safe for aircraft. However, the disruption to transatlantic and European aviation during the first week of explosive activity at Eyjafjallajökull (14–18 April 2010) led to a relaxation of this policy in Europe, with the UK Civil Aviation Authority and Eurocontrol introducing ash concentration thresholds for commercial air traffic [*Bonadonna et al.*, 2012]. Ash concentrations below $2 \, \mathrm{mg} \, \mathrm{m}^{-3}$ are considered safe for flights [*ICAO*, 2010; *CAA*, 2011; *Langmann et al.*, 2012], while flight operations at higher concentrations require a Safety Case accepted by national regulators [*CAA*, 2011]. Typically, Safety Cases have been accepted for ash concentrations up to $4 \, \mathrm{mg} \, \mathrm{m}^{-3}$ [*CAA*, 2011]. The introduction of ash concentration levels places increased demands on atmospheric ash dispersion modeling for airspace management during volcanic crises [*Bonadonna et al.*, 2012]. Crucial components of forecasts of the movement of ash in the atmosphere are the level of neutral buoyancy of the volcanic plume in the stratified atmosphere (the 'plume height') and the mass flux of material released from the volcano. Accurately determining these source conditions is an essential requirement for airspace management during volcanic crises [*Bonadonna et al.*, 2012].

[4]   The source mass flux of a volcanic plume is currently impossible to measure directly but is fundamentally related to the plume height as a result of the dynamics of buoyant

[1]School of Mathematics, University of Bristol, Bristol, UK.
[2]School of Earth Sciences, University of Bristol, Bristol, UK.

Corresponding author: M. J. Woodhouse, School of Mathematics, University of Bristol, Bristol BS8 1TW, UK. (mark.woodhouse@bristol.ac.uk)

plume rise in the atmosphere [*Morton et al.*, 1956]. This has led to inversion methods to estimate the source mass flux based on the approximate quarter-power relationship to the plume height in a density-stratified environment such as the atmosphere [*Morton et al.*, 1956; *Wilson et al.*, 1978; *Sparks*, 1986; *Sparks et al.*, 1997; *Mastin et al.*, 2009]. A small dataset of historic eruptions where the source duration, total erupted mass, and plume neutral buoyancy height are known has been used to calibrate this relationship [*Wilson et al.*, 1978; *Sparks*, 1986; *Sparks et al.*, 1997; *Mastin et al.*, 2009]. This dataset (and the calibrated plume height-mass flux relationship) is inevitably biased by the disproportionate number of large eruption events, for which volcanic ash deposits are more easily assessed, while there is less data available for the more frequent yet smaller eruptions. Furthermore, plumes from smaller eruptions are more strongly affected by atmospheric conditions, in particular atmospheric winds, during the ascent of material in the atmosphere. Wind-affected volcanic plumes are therefore under-represented in the historical eruption dataset, so application of calibrated inversion methods to lower source mass flux plumes produced by smaller magnitude volcanic activity could be significantly in error. We have re-analyzed the historic eruption dataset and find that volcanic plume height depends systematically on atmospheric wind speed for a given source flux, and have explored the underlying relationships using an integral modeling approach accounting for the thermodynamic exchange of heat between volcanic ash, volcanic gas, and entrained atmospheric air, and the entrainment of horizontal momentum due to the atmospheric wind [*Hewett et al.*, 1971; *Bursik*, 2001].

[5] The key physical process controlling the ascent of a turbulent buoyant plume is the entrainment of environmental fluid into the body of the plume by turbulent eddies on the plume margins. Turbulence within the plume then efficiently mixes the entrained fluid, altering the density contrast between the plume and the surrounding environment. In a stratified environment, the plume density may eventually match that of the environment, at which point the vertical component of the buoyancy force on the plume vanishes. This is the level of neutral buoyancy. Inertia causes the plume to rise above this level of neutral buoyancy, and the plume density here exceeds the environment. The material in the plume therefore falls back and begins to spread laterally about the level of neutral buoyancy.

[6] Integral models of turbulent buoyant plumes [*Morton et al.*, 1956] represent the entrainment process through a simple entrainment velocity which, in the most basic models, is linearly proportional to the centerline velocity of the plume with the coefficient of proportionality known as the entrainment coefficient, here denoted by k_s. Such models have been utilized widely to quantitatively describe the rise of industrial and environmental plumes [*Woods*, 2010]. An integral model of volcanic eruption columns can be formulated by explicitly including a description of the thermodynamics of heat transfer between solid pyroclasts, magmatic gases, and entrained air [*Woods*, 1988].

[7] Plume rise in a crosswind has been modeled by including momentum conservation in the horizontal direction as well as the vertical [*Hewett et al.*, 1971]. The wind-driven plume model introduces an additional entrainment coefficient, denoted here by k_w, which parameterizes the entrainment parallel to the plume as it bends over in the crosswind. Together, these models can be used to describe the rise of volcanic eruption columns in a wind field [*Bursik*, 2001; *Degruyter and Bonadonna*, 2012].

[8] Eyjafjallajökull is a stratovolcano on the south coast of Iceland, with a summit at 1666 m above sea level [*Siebert and Simkin*, 2002–2012]. The 2.5 km-wide summit caldera is covered by ice around 200 m (and up to 400 m) thick [*Magnússon et al.*, 2012]. The explosive phases of the Eyjafjallajökull eruption began on 14 April 2010 beneath the ice cover. Volcano-ice interactions rapidly melted through the ice cover, with distinct cauldrons forming during 14–16 April [*Magnússon et al.*, 2012]. An ash-poor plume from Eyjafjallajökull was observed on the morning of 14 April [*Arason et al.*, 2011; *Höskuldsson et al.*, 2011; *Magnússon et al.*, 2012], with a dark ash-rich plume rising from around 1830 UTC on 14 April and continuing until 18 April. The volcano-ice interaction during the first explosive phase (14–17 April) produced very fine-grained ash [*Dellino et al.*, 2012]. Between 18 April and 4 May, the eruption intensity fell, but explosive activity resumed on 5 May and continued with a varying intensity until 18 May (the second explosive phase) [*Gudmundsson et al.*, 2011; *Höskuldsson et al.*, 2011] producing fine-grained ash-rich plumes. From 18 May, the eruption intensity declined, with continuous activity ending on 22 May 2010. Some of the fine-grained ash, produced predominately during the first explosive phase and the early part of the second explosive phase (5–7 May) [*Stevenson et al.*, 2012], was carried over large distances by atmospheric winds, although most was deposited near to the volcano as aggregates [*Bonadonna et al.*, 2011; *Stevenson et al.*, 2012].

[9] In section 2, we derive an integral model to describe volcanic plumes, composed of solid pyroclasts, magmatic gases, and entrained air, rising in a windy atmosphere. We demonstrate that the predictions of the integral model for the dependence of the plume rise height on the source mass flux adequately describe observations from the historical record when wind shear is included in the integral model. The integral model predictions are used to calibrate a new semi-empirical relationship, akin to those of *Sparks et al.* [1997] and *Mastin et al.* [2009], that explicitly includes the atmospheric wind speed. In order to assess the role of phase changes of water and the release of latent heat on the ascent of wind-blown volcanic plumes, we derive an integral model of moist volcanic plumes in a windy, moist atmosphere in section 3. We discuss the implications of our modeling in sections 4 and 5. In section 4, we compare results of our integral plume models to a time series of observed plumes rise heights during the first explosive phase of the 2010 Eyjafjallajökull eruption. We demonstrate that the inclusion of atmospheric wind in the integral plume model allows observed variations in plume height to be described, with significant implications for the estimation of the source mass flux. We then comment on the consequences of our results for ash dispersion modeling and aviation, and on the estimation of the source mass
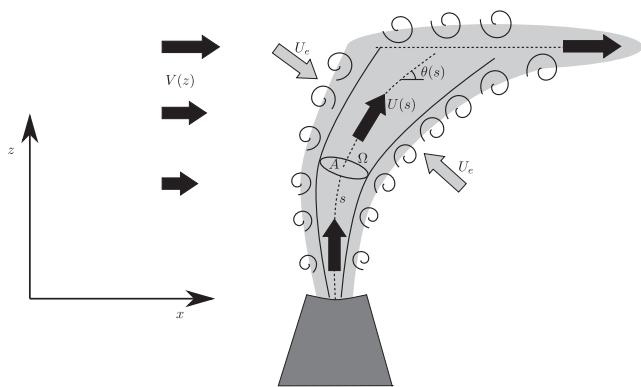
Figure 1. A model of a volcanic plume in a crosswind. A Cartesian coordinate system is fixed with x denoting the distance downwind from the vent and z denoting the vertical distance from the vent. Equations describing the plume dynamics are derived in a plume-centered coordinate system, with s denoting the curvilinear distance (arc length) from the vent along the plume axis, and $\theta(s)$ is the angle of the centerline with respect to the horizontal. A cross-section of the plume normal to the centerline has area A and circumference Ω. The wind speed is denoted by $V(z)$, the centerline speed of the plume is $U(s)$, and U_e denotes the entrainment velocity at the plume margins.

flux for explosive volcanic eruptions, in section 5. Finally, in section 6, we present some concluding remarks.

2. Integral Model of Dry Volcanic Eruption Columns in a Crosswind

[10] An integral model for a steady volcanic eruption column in a wind field can be derived by combining an integral model of pure plumes in a horizontal wind [*Hewett et al.*, 1971] with an integral model of volcanic eruption columns in a quiescent atmosphere [*Woods*, 1988]. The volcanic plume model of *Woods* [1988] extends the classical integral model of turbulent buoyant plumes [*Morton et al.*, 1956] to include essential features of volcanic eruption columns. In particular, aspects of the multiphase character of the plume, which is a mixture of solid pyroclasts and gases, and the thermodynamics of heat exchange between these phases are included in the mathematical description of the plume.

[11] The mathematical model presented here shares the same entrainment formulation [*Hewett et al.*, 1971] as that applied by *Bursik* [2001] to volcanic plumes. However, while *Bursik* [2001] adopts the quiescent plume model of *Glaze and Baloga* [1996], our model utilizes the formulation of *Woods* [1988] which additionally incorporates the influence of the solid pyroclasts on the bulk plume properties (i.e., the plume density and heat capacity) and so is applicable for large explosive eruptions where the solid content of the plume near the vent is high and the heat content of the pyroclasts and transfer of heat from solids to entrained air has an important effect on the plume dynamics [*Woods*, 1988; *Sparks et al.*, 1997]. The model of *Woods* [1988] neglects the contribution of the adiabatic cooling of the gas phase in the energy conservation equation that appears in the model of *Glaze and Baloga* [1996] for vapor plumes.

The adiabatic cooling term [*Glaze and Baloga*, 1996] is typically much smaller than the cooling produced by the entrainment of ambient atmospheric air, making only a small contribution to the heat budget. Furthermore, it is not clear how the presence of solid pyroclasts affects this adiabatic cooling, particularly at high solids concentration near to the vent. While a significant proportion of the gas issuing from volcanic vents is water vapor [*Sparks et al.*, 1997], in this section we assume there is no change of phase of the water vapor, an assumption that is relaxed in section 3 where we develop an extension of the dry wind-blown plume model to describe the moisture content of the plume and the surrounding environment.

[12] Models of the fallout of pyroclasts from the rising plume have been proposed for plumes in quiescent environments [*Ernst et al.*, 1996; *Woods and Bursik*, 1991; *Sparks et al.*, 1997]. However, it is not currently known how the interaction with the wind modifies the empirical settling models [*Ernst et al.*, 1996; *Bursik*, 2001] that are used to describe sedimentation of particles from plumes rising in quiescent environments. Plume models which include particle fallout in quiescent environments have shown that the loss of mass associated with fallout has only a small effect on the rise height attained by buoyant plumes unless fallout occurs before pyroclasts have thermally equilibrated with the gases in the plume [*Woods and Bursik*, 1991; *Sparks et al.*, 1997]. For eruptions producing pyroclasts larger than a few millimeters, there is a significant relaxation time to thermal equilibrium and pyroclasts may fall out before thermal equilibrium is reached, reducing the supply of heat (and therefore buoyancy) to the eruption column [*Woods and Bursik*, 1991; *Sparks et al.*, 1997]. Therefore, for coarse-grained eruption columns, particle fallout may play an important role in determining the plume rise height. In contrast, since thermal equilibrium occurs rapidly for small grain sizes (within 1 km of the vent for pyroclasts of diameter up to approximately 0.4 cm ejected at $100 \, \mathrm{m \, s^{-1}}$) [*Woods and Bursik*, 1991; *Sparks et al.*, 1997], the fallout of pyroclasts has little effect on fine-grained eruption columns. We expect thermal equilibration of the fine-grained pyroclasts and the gases to also occur rapidly in a wind-blown plume, so expect the fallout of pyroclasts to have only a secondary effect on the rise height attained by the plume. We therefore neglect the fallout of pyroclasts in our model.

[13] The entrainment of environmental air into the body of the plume through the action of turbulent eddies is parameterized empirically by an entrainment velocity that is directed normal to the local plume axis (Figure 1). In a windy environment, where the plume trajectory deviates from the vertical, the entrainment velocity has contributions from the differential velocities tangential and normal to the axis of the plume. This can be modeled [*Hewett et al.*, 1971] with an entrainment velocity given by

$$U_e = k_s|U - V\cos\theta| + k_w|V\sin\theta|, \qquad (1)$$

where U is the axial centerline velocity of the plume, V is the horizontal velocity of the wind, θ is the local angle of the plume axis to the horizontal, k_s is the entrainment coefficient due to the motion of the plume relative to the environment, and k_w is the entrainment coefficient due to the alignment of the wind field with the local normal to the plume axis.

In the absence of atmospheric wind, $V = 0$, the entrainment velocity (1) reduces to $U_e = k_s U$, and therefore, k_s is the entrainment coefficient for plumes rising in a quiescent environment [Morton et al., 1956; Woods, 1988]. When incorporated into an integral model of buoyant plumes in a uniform crosswind, this form for the entrainment velocity (1) is able to reproduce plume trajectories observed in laboratory experiments [Hewett et al., 1971].

[14] A mathematical description of the variation of the steady eruption column with distance from the volcanic source is formulated in a plume-centered coordinate system within a Cartesian frame of reference (Figure 1). We let z denote the height of the plume, x denote the distance from the vent in the downwind direction and s denote the curvilinear distance from the vent along the centerline of the plume. Therefore, x and z are related to s through

$$\frac{\mathrm{d}x}{\mathrm{d}s} = \cos\theta, \quad \frac{\mathrm{d}z}{\mathrm{d}s} = \sin\theta. \tag{2}$$

[15] Turbulence within the body of the plume ensures that the material remains well mixed, and properties of the eruption column can be described by time-averaged bulk quantities, with the time averaging performed over a time interval greater than the eddy-turnover time [Woods, 1988]. The bulk density of the plume, denoted by $\rho(s)$, varies due to the entrainment, mixing, and expansion of atmospheric air, which has density ρ_a. The bulk temperature of the column is denoted by $T(s)$, while the atmospheric temperature is T_a. Equations describing the variation of $\rho(s)$, $U(s)$, and $T(s)$ are derived by considering conservation of mass, momentum, and energy in cross-sections normal to the plume axis with area A and boundary Ω (Figure 1). Neglecting the fallout of solid pyroclasts from the column, the mass of the column increases due to the entrainment of atmospheric air at the boundary of the plume, so mass conservation demands

$$\frac{\mathrm{d}}{\mathrm{d}s} \int \rho U \, \mathrm{d}A = \oint \rho_a U_e \mathrm{d}\Omega. \tag{3}$$

[16] An equation for the conservation of vertical momentum can be written using Newton's second law, with the change in vertical momentum balancing the buoyancy force,

$$\frac{\mathrm{d}}{\mathrm{d}s} \int \rho U^2 \sin\theta \mathrm{d}A = \int g(\rho_a - \rho)\mathrm{d}A. \tag{4}$$

Here it is assumed that deviations of the vertical pressure gradient from hydrostatic and stresses are negligible. The horizontal momentum of the column changes only due to the entrainment of fluid from the windy environment, so conservation of horizontal momentum can be written

$$\frac{\mathrm{d}}{\mathrm{d}s} \int \rho U^2 \cos\theta \mathrm{d}A = \oint \rho_a U_e V \mathrm{d}\Omega. \tag{5}$$

[17] It is most convenient to formulate the total energy of the eruption column at distance s in terms of the bulk enthalpy of the plume material [Woods, 1988], as the work done in expanding gaseous phases due to temperature or pressure changes is then included. The total energy of the plume is the sum of the bulk enthalpy, kinetic energy and potential energy, and the total energy changes due to the entrainment of atmospheric fluid. Conservation of energy is therefore given by

$$\frac{\mathrm{d}}{\mathrm{d}s} \int \rho \left(C_p T + \frac{U^2}{2} + gz \right) U \mathrm{d}A$$
$$= \oint \rho_a \left(C_a T_a + \frac{U_e^2}{2} + gz \right) U_e \mathrm{d}\Omega, \tag{6}$$

where C_p and C_a are the specific heat capacities at constant pressure of the bulk plume and the atmospheric air, respectively.

[18] If we assume top-hat profiles for ρ, U, and T (i.e., these quantities have constant values within the plume and vanish outside the plume boundary) and that cross-sections of the plume normal to the axis are circular with radius $R(s)$, then the integrals in (3)–(6) can be evaluated to give

$$\frac{\mathrm{d}}{\mathrm{d}s} (\rho U R^2) = 2\rho_a U_e R, \tag{7}$$

$$\frac{\mathrm{d}}{\mathrm{d}s} (\rho U^2 R^2 \sin\theta) = (\rho_a - \rho)gR^2, \tag{8}$$

$$\frac{\mathrm{d}}{\mathrm{d}s} (\rho U^2 R^2 \cos\theta) = 2\rho_a U_e R V, \tag{9}$$

$$\frac{\mathrm{d}}{\mathrm{d}s} \left(\rho U R^2 \left(C_p T + \frac{U^2}{2} + gz \right) \right)$$
$$= 2\rho_a R U_e \left(C_a T_a + \frac{U_e^2}{2} + gz \right). \tag{10}$$

Other profiles, for example, Gaussian distributions, could be adopted to describe the variation of density, velocity, and temperature within the plume. However, adopting such profiles has little effect on the predictions of plume models in quiescent environments if the value of the entrainment coefficient is appropriately adjusted [Kaye, 2008].

[19] The mass flux πQ, axial momentum flux πM, and the enthalpy flux πE of the eruption column are defined as

$$Q = \rho U R^2, M = \rho U^2 R^2, E = \rho U R^2 C_p T. \tag{11}$$

The system of equations (7)–(10) can be combined to give

$$\frac{\mathrm{d}Q}{\mathrm{d}s} = 2\rho_a U_e \frac{Q}{\sqrt{\rho M}}, \tag{12}$$

$$\frac{\mathrm{d}M}{\mathrm{d}s} = g(\rho_a - \rho)\frac{Q^2}{\rho M}\sin\theta + 2\rho_a \frac{Q}{\sqrt{\rho M}} U_e V \cos\theta, \tag{13}$$

$$\frac{\mathrm{d}\theta}{\mathrm{d}s} = g(\rho_a - \rho)\frac{Q^2}{\rho M^2}\cos\theta - 2\rho_a \frac{Q}{M\sqrt{\rho M}} U_e V \sin\theta, \tag{14}$$

$$\frac{\mathrm{d}E}{\mathrm{d}s} = \left(C_a T_a + \frac{U_e^2}{2} \right)\frac{\mathrm{d}Q}{\mathrm{d}s} + \frac{M^2}{2Q^2}\frac{\mathrm{d}Q}{\mathrm{d}s}$$
$$- \frac{\rho_a}{\rho} Q g \sin\theta - 2\rho_a \sqrt{\frac{M}{\rho}} U_e V \cos\theta, \tag{15}$$

95

where

$$U_e = k_s \left| \frac{M}{Q} - V\cos\theta \right| + k_w |V\sin\theta|. \qquad (16)$$

[20] The bulk density of the plume is related to the density of the solids pyroclasts, ρ_s, and the density of the gaseous phase [Woods, 1988] as

$$\frac{1}{\rho} = \frac{1-n}{\rho_s} + \frac{nR_gT}{P_a}, \qquad (17)$$

where n is the mass fraction of gas, P_a is the pressure of the atmosphere, and R_g is the bulk gas constant of the plume. Note that in (17), it is assumed that the pressure in the plume is instantly equilibrated with the atmospheric pressure. Conservation of solid pyroclasts, with no particle fallout, allows the gas mass fraction to be determined as

$$n = 1 - (1-n_0)\frac{Q_0}{Q}, \qquad (18)$$

where zero subscripts denote quantities at the vent. The bulk gas constant and bulk heat capacity at constant pressure can then be determined [Woods, 1988; Scase, 2009] with

$$R_g = R_a + (R_{g0} - R_a)\frac{n_0(1-n)}{n(1-n_0)}, \qquad (19)$$

$$C_p = C_a + (C_{p0} - C_a)\frac{(1-n)}{(1-n_0)}, \qquad (20)$$

where R_a and C_a are the gas constant and the heat capacity at constant pressure of the air, respectively. We assume that the magmatic gas at the vent is composed predominately of water vapor, so take the bulk gas constant at the source to be the gas constant of water vapor, $R_{g0} = R_v$, and the bulk specific heat capacity to be given by $C_{p0} = n_0 C_v + (1 - n_0)C_s$, where C_v and C_s are the specific heat capacities at constant pressure of water vapor and the solid pyroclasts, respectively.

[21] If observations of the atmospheric temperature and pressure are known, they can be utilized in the plume model, with interpolation between data points used to approximate the atmospheric conditions at points of integration. Here we use linear interpolation as this does not introduce possibly spurious local extrema in the atmospheric fields. In the absence of atmospheric observations, we adopt the U.S. Standard Atmosphere [COESA, 1976] to describe the atmospheric temperature and pressure fields, with the atmospheric temperature given by

$$T_a(z) = \begin{cases} T_{a0} - \mu z, & \text{for } z < H_1, \\ T_{a0} - \mu H_1, & \text{for } H_1 \le z \le H_2, \\ T_{a0} - \mu H_1 + \lambda(z - H_2), & \text{for } z > H_2, \end{cases} \qquad (21)$$

where T_{a0} is the temperature at sea level, μ and λ are the lapse rates of temperature in the troposphere and stratosphere, respectively, H_1 is the altitude at which the tropopause begins, and H_2 is the altitude at which the stratosphere begins. Note that the temperature in the Standard Atmosphere decreases linearly in the troposphere and increases

linearly in the stratosphere. The atmospheric pressure in the Standard Atmosphere is assumed to be hydrostatic [Gill, 1982],

$$\frac{dP_a}{dz} = -\frac{gP_a}{R_aT_a}. \qquad (22)$$

The density of the atmosphere is found by assuming that the atmospheric gases behave as ideal gases, so

$$\rho_a = \frac{P_a}{R_aT_a}. \qquad (23)$$

[22] The mathematical model is completed by providing closure relations for the entrainment coefficients. Typically, the entrainment coefficient for buoyant plumes in quiescent environments is taken to be a constant, with $k_s \approx 0.09$. However, there is some evidence from laboratory experiments that k_s is not constant [Kaye, 2008] but varies towards a constant value as the plume evolves towards a self-similar form [Kaminski et al., 2005; Carazzo et al., 2006]. The variation in the entrainment coefficient is related to the profiles of plume velocity, buoyancy, and turbulent shear stress within the plume, and an empirical expression for the entrainment coefficient has been determined for plumes in a quiescent environment [Carazzo et al., 2006]. In a cross flow, it is likely that these profiles are altered. However, there has been no investigation of the detailed influence of the wind on the variation of the entrainment coefficient. We therefore adopt a simple model [Woods, 1988] to represent the variation of the entrainment coefficient as the eruption column develops from a momentum-driven jet near the vent to a buoyant plume, with the eruption column separated into distinct regions. In the near-source region, the material issuing from the vent is more dense than the atmosphere due to the high concentration of particulates and is driven upwards as a dense jet. The entrainment coefficient in this gas-thrust region is a function of the density contrast [Woods, 1988] and is taken to be $k_s = \sqrt{\rho/\rho_a}/16$. The entrainment of atmospheric air in the gas-thrust region reduces the bulk density of the eruption column and may lead to the column becoming buoyant. In this buoyant region, we take the entrainment coefficient $k_s = 0.09$. There have been fewer investigations of appropriate entrainment models for plumes in a crosswind. A study of the sensitivity of model predictions for the rise height of volcanic plumes in a wind field to the values assigned to the entrainment coefficients [Barsotti et al., 2008] has shown that variation in the entrainment coefficients, within the range $0.09 \le k_s \le 0.15$ and $0.6 \le k_w \le 1.0$ suggested by experimental investigations, results in significant changes in the calculated plume heights. Here we take a constant entrainment coefficient $k_w = 0.9$ determined from a series of laboratory experiments [Hewett et al., 1971].

[23] Examples of solutions of the integral model for volcanic plumes in a crosswind, with atmospheric conditions modeled with the U.S. Standard Atmosphere and parameters given in Table 1, are shown in Figure 2. Initial conditions for the integration of the governing equations are given in Table 2. The atmospheric wind profile is modeled with a

Table 1. Parameters Employed in the Dry Volcanic Plume Model

Parameter	Symbol	Value	Unit
Atmospheric pressure at sea level	P_{a0}	100	kPa
Atmospheric temperature at sea level	T_{a0}	293	K
Density of solid pyroclasts	ρ_s	1200	$\mathrm{kg\,m^{-3}}$
Entrainment coefficient in absence of wind	k_s	0.09	
Entrainment coefficient due to wind	k_w	0.9	
Gas constant of atmosphere	R_a	285	$\mathrm{J\,K^{-1}\,kg^{-1}}$
Gas constant of volcanic gas at vent	R_{g0}	462	$\mathrm{J\,K^{-1}\,kg^{-1}}$
Gravitational acceleration	g	9.81	$\mathrm{m\,s^{-2}}$
Height of stratosphere	H_2	20	km
Height of tropopause	H_1	11	km
Lapse rate of temperature in stratosphere	λ	2.0	$\mathrm{K\,km^{-1}}$
Lapse rate of temperature in troposphere	μ	6.5	$\mathrm{K\,km^{-1}}$
Specific heat capacity of atmosphere	C_a	998	$\mathrm{J\,K^{-1}\,kg^{-1}}$
Specific heat capacity of column at vent	C_{p0}	1624	$\mathrm{J\,K^{-1}\,kg^{-1}}$

constant wind shear up to the tropopause, with constant wind speed V_1 above,

$$V(z) = \begin{cases} V_1 z / H_1, & \text{for } z < H_1, \\ V_1, & \text{for } z \geq H_1. \end{cases} \quad (24)$$

[24] The solutions demonstrate increasingly bent-over plume trajectories as the wind speed V_1 increases.
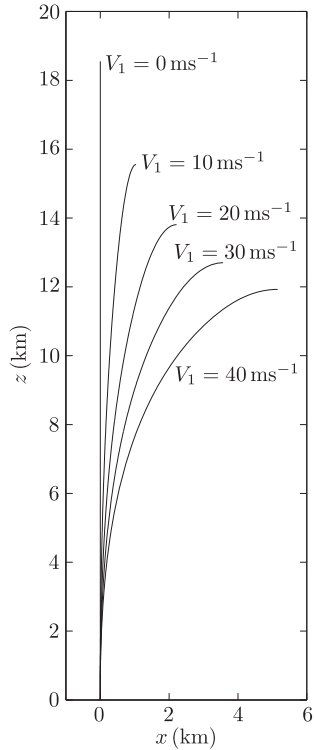
Figure 2. Calculated centerline trajectories of volcanic plumes in a crosswind. The wind is taken to increase linearly in the troposphere to a speed V_1 at height $z = 11$ km and has constant speed above. We take $V_1 = 0$ (with $\mathcal{W}_s = 0$ as defined in equation 26), $V_1 = 10\,\mathrm{m\,s^{-1}}$ ($\mathcal{W}_s = 0.09$), $V_1 = 20\,\mathrm{m\,s^{-1}}$ ($\mathcal{W}_s = 0.17$), $V_1 = 30\,\mathrm{m\,s^{-1}}$ ($\mathcal{W}_s = 0.26$), and $V_1 = 40\,\mathrm{m\,s^{-1}} (\mathcal{W}_s = 0.34)$. The temperature profile of the atmosphere is modeled using the U.S. Standard Atmosphere [COESA, 1976]. The complete set of model parameters is provided in Table 2.

Furthermore, the enhanced entrainment of environmental fluid into a plume rising in a wind field results in a more rapid rate of decrease in the density contrast between the plume and the atmosphere, and the rise height of the plume in a crosswind is consequently reduced. Note here we have not considered rotation of the wind field. The integral plume model can be extended to include changing wind direction by introducing a third coordinate axis, the azimuthal wind angle, and an additional equation for the conservation of momentum along this third axis. An examination of solutions to the integral model in wind fields with varying direction (not shown here) suggests that rotation of the wind vector has little effect on the rise height of volcanic eruption columns since the entrainment velocity is dependent on the wind speed but not on the wind direction and a changing wind direction usually does not add significantly to the length of the trajectory of the ascending plume.

2.1. Comparison of Model Predictions to Observations

[25] We have re-analyzed the record of plume rise height and mass flux of historic eruptions [Sparks et al., 1997; Mastin et al., 2009] to investigate the effect of atmospheric wind. For some of the eruptions in the dataset, typical wind speeds at the time of the eruption (as recorded in the Smithsonian Institution Global Volcanism Program database [Siebert and Simkin, 2002–2012]) can be estimated from ECMWF reanalysis meteorological data (ECMWF ERA-Interim data have been obtained from the ECMWF Data Server) (Figure 3). There is a degree of scatter in the data, some of which could be attributed to varying atmospheric conditions, for example, the variation in atmospheric lapse rates and altitude of atmospheric layers with latitude, which are known to influence rise heights of volcanic plumes [Woods, 1995; Sparks et al., 1997]. In addition, by adopting the wind speed at a single altitude to characterize the atmospheric wind conditions, we are unable to describe atmospheric wind structures, such as jet streams, which may have a significant influence on the ascent of the plume [Bursik, 2001; Bursik et al., 2009]. However, despite these limitations, we find that the dataset records a systematic dependence of volcanic plume height on atmospheric wind speed for a given source mass flux (Figure 3). In particular, at high wind speeds in excess of $30\,\mathrm{m\,s^{-1}}$, plume heights tend to be limited to altitudes below 15 km.

[26] The predictions of our model for the variation of plume height with source mass flux for increasing atmospheric wind speed are shown in Figure 3. Here the atmospheric wind is modeled as a linear shear flow in the tropopause with constant wind speed above (24), and the atmospheric temperature is described using the U.S. Standard Atmosphere (21) [COESA, 1976]. A range of exit velocities and vent radii

Table 2. Source Conditions for Example Profiles of Dry Volcanic Plumes in a Crosswind (Figure 2)

Variable	Symbol	Value	Unit
Column temperature	T_0	1200	K
Exit angle	θ_0	0	
Exit velocity	U_0	100	$\mathrm{m\,s^{-1}}$
Gas mass fraction	n_0	0.03	
Vent altitude	z_0	0	m
Vent radius	R_0	100	m
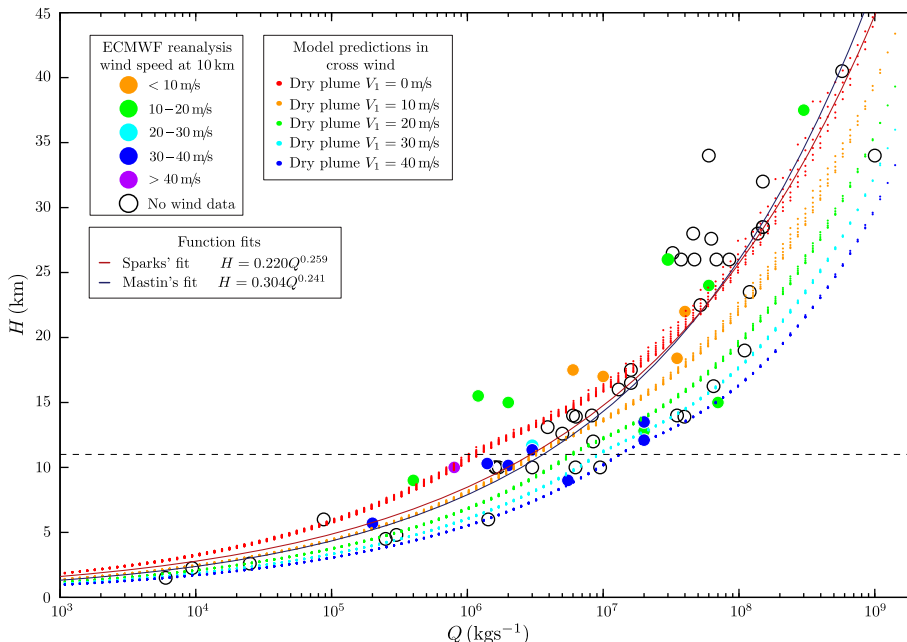
Figure 3. The rise height of an eruption column, H, as a function of the mass flux of material from the volcanic vent, Q. A data set of historical eruptions [*Sparks et al.*, 1997; *Mastin et al.*, 2009] where the mass flux of the eruption, Q, and rise height of the plume, H, can be independently estimated is used to calibrate a scaling law relationship between rise height and mass flux [*Sparks et al.*, 1997; *Mastin et al.*, 2009] (as given on the figure, for H measured in km and Q measured in $\mathrm{kg\,s^{-1}}$). A representative wind speed at an altitude of 10 km can be assigned, in some cases, using ECMWF Reanalysis data. The data show a tendency for plume rise heights from small eruptions (source mass flux $Q < 10^8$ $\mathrm{kg\,s^{-1}}$) to be reduced in high winds (wind speed $V_1 > 20\,\mathrm{m\,s^{-1}}$). Predictions of the integral model of dry volcanic plumes in a crosswind that increases linearly with altitude up to a speed V_1 at the tropopause at an altitude of 11 km (denoted by the black dashed line) are computed using the U.S. Standard Atmosphere [*COESA*, 1976] to describe the temperature profile in the atmosphere, for a range of exit velocities and vent radii (the source conditions employed are given in Table 3).

are employed as given in Table 3 together with the other model parameter values used. The model predictions reproduce the expected quarter-power scaling between the rise height and the source mass flux, particularly for large source mass flux. A deviation from the approximate quarter-power scaling is observed for smaller source mass flux, which is particularly apparent for low wind speeds, when the plumes reach the tropopause where there is a discontinuous change in the atmospheric lapse rate. If a constant wind speed is adopted in the volcanic plume model, the model over-predicts the reduction in plume rise height for a specified source mass flux when compared to the observations (these calculations are not shown here). However, when the vertical profile of wind shear is accounted for, there is improved agreement between the model predictions and the observational dataset (Figure 3).

[27] Curve fits calibrated to observations of historical eruptions [*Sparks et al.*, 1997; *Mastin et al.*, 2009] (Figure 3) do not explicitly account for crosswinds on the rise of volcanic plumes. Figure 3 demonstrates the strong influence of atmospheric winds on the ascent of volcanic plumes. For small and moderately sized eruptions, a strong crosswind can limit the plume rise height such that the source mass flux estimated using the calibrated curve fits [*Sparks et al.*, 1997;

Mastin et al., 2009] are underpredicted by an order of magnitude [see also *Bursik*, 2001].

2.2. Relating Mass Flux and Rise Height for Wind-blown Plumes

[28] The transition from strong plumes that are little affected by the wind field during their ascent to weak plumes with trajectories that are strongly bent over can be quantified using a dimensionless parameter

$$\mathcal{W}_p = \frac{k_s^{1/2} V}{\left[\dfrac{g}{\rho_{a0}}\left(\dfrac{C_p T - C_a T_a}{C_a T_a}\right)Q\right]^{1/4} N^{1/4}}, \qquad (25)$$

where V is a representative wind speed, ρ_{a0} is the density of the plume at the source, T and T_a are the temperature of the plume and environment, respectively, at the source, C_p and C_a are the specific heat capacities at constant pressure of the plume and environment, respectively, g is the acceleration due to gravity, and N is the buoyancy frequency of the atmosphere. The parameter $\mathcal{W}_p$ represents the ratio of the horizontal wind speed to the vertical buoyant rise speed, assuming the wind speed is uniform with altitude. However, taking a uniform wind may not be representative of

Table 3. Source Conditions Employed in Model Predictions for Rise Height of Volcanic Plumes in a Crosswind (Figure 3)

Variable	Symbol	Value	Unit
Column temperature	T_0	1200	K
Exit angle	θ_0	0	
Exit velocity	U_0	1–500	$m\,s^{-1}$
Gas mass fraction	n_0	0.05	
Vent altitude	z_0	0	m
Vent radius	R_0	1–500	m

atmospheric winds. The atmospheric wind can be usefully approximated as a linear shear flow in the lower atmosphere, taking $V(z) = \dot{\gamma}z$ where $\dot{\gamma}$ is the shear rate and z is the height in the atmosphere. In a shear flow, dimensional analysis shows the appropriate dimensionless parameter measuring the strength of the wind field is

$$\mathcal{W}_s = \frac{\dot{\gamma}}{N} = \frac{V_1}{NH_1}, \qquad (26)$$

where $V_1 = V(H_1)$ is the wind speed at a reference altitude H_1 (e.g., at the tropopause) (see also Appendix A). We note that the dimensionless parameter $\mathcal{W}_s$ depends only on properties of the atmosphere and is independent of the plume source conditions. The parameter $\mathcal{W}_s$ can be interpreted as the ratio of the time scale of vertical motions, given by $1/N$, to the timescale of horizontal motions, $1/\dot{\gamma}$. Thus, for $\mathcal{W}_s \gg 1$, horizontal motion of a parcel of fluid in the plume, induced by the wind, occurs on shorter time scales than the vertical rise of the parcel in the plume and so the plume trajectory bends over in the wind, while for $\mathcal{W}_s \ll 1$, the vertical motion occurs on a shorter time scale than the horizontal motion and there is little deviation of the plume trajectory from the vertical. A similar dimensionless parameter has been identified by *Degruyter and Bonadonna* [2012], where the column-averaged wind speed and buoyancy frequency are adopted. Here a local wind speed and reference height are taken in order to represent the vertical shear profile of the atmospheric wind. Solutions of the integral plume model in a crosswind demonstrate the controlling influence of $\mathcal{W}_s$ (Figure 2). For explosive eruptions of the magnitude of Eyjafjallajökull 2010 and a wind speed of $V_1 = 40\,ms^{-1}$ at $H_1 = 10$ km, the parameter $\mathcal{W}_s = 0.4$, taking an atmospheric buoyancy frequency $N = 0.01\,s^{-1}$. In order to obtain weak plumes, $\mathcal{W}_s > 1$, very strong wind shear or weak atmospheric stratification is required. However, variations in the vertical rise speed, wind speed, and temperature profile cause local variations in the plume strength. In particular, as the plume decelerates as it nears the level of neutral buoyancy, the wind field will inevitably cause a bending over of the plume trajectory as the maximum altitude is approached (Figure 2). Furthermore, it is not appropriate to represent the wind profile as a linear shear throughout the atmosphere, and for larger eruptions, with plumes that ascend above the troposphere, there may be interaction with jet streams where the wind speed is locally high [*Bursik*, 2001; *Bursik et al.*, 2009]. While any profile of the wind could be used, for small and moderately sized eruptions that do not rise significantly above the troposphere and where the wind field can be taken to increase linearly with altitude, the parameter $\mathcal{W}_s$ is appropriate to assess the strength of the wind.

[29] An estimate of the effect of the shear rate on the rise height of volcanic plumes can be obtained from a simple integral model of pure plumes rising in a linear shear cross flow, as described in Appendix A. In the pure plume model, the multiphase character of volcanic plumes and the thermodynamics of the gas expansion are not considered. Furthermore, the atmosphere is assumed to be uniformly stratified. Numerical solutions for pure plumes in a linear shear flow can be readily calculated and the rise height of pure plumes determined (Figure 4). From the numerical solutions (as detailed in Appendix A), a rational function approximation can be used to describe the effect of the parameter $\mathcal{W}_s$ on the rise height. We find that the rise height above the vent is well described by

$$H \approx H_0 \frac{1 + 1.373\mathcal{W}_s}{1 + 4.266\mathcal{W}_s + 0.3527\mathcal{W}_s^2}, \qquad (27)$$

where H_0 is the rise height of a pure plume in a quiescent environment. This approximation adequately reproduces the numerical solution of the pure plume model for $\mathcal{W}_s < 5$ (Figure 4), so the approximation is appropriate for typical atmospheric conditions.

[30] An approximation of the rise height for volcanic plumes in a quiescent atmosphere that remain within the troposphere can be found from a fit to data obtained from the integral plume model in a Standard Atmosphere as

$$H_0 \approx 0.318Q^{0.253}, \qquad (28)$$

for rise height H_0 measured in kilometer and source mass flux Q measured in kilogram per second, which is similar to the expressions obtained from fits to observational data
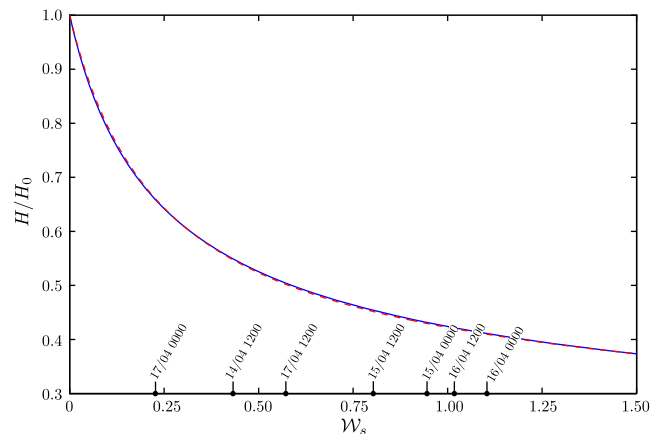
Figure 4. The height of neutral buoyancy for pure plumes in a linear shear flow as a function of the wind strength parameter $\mathcal{W}_s$ (blue solid line). The height of neutral buoyancy, H, is normalized by the height of neutral buoyancy for a pure plume in a quiescent environment, H_0. The ambient environment is uniformly stably stratified. A rational function approximation, equation (27), with three fitting parameters, well describes the numerically determined relationship for $\mathcal{W}_s \leq 5$ (red dashed line). Values of $\mathcal{W}_s$ estimated for Eyjafjallajökull 14–17 April 2010 using radiosonde measurements of the meteorology at Keflavik International Airport [*Oolman*, 2012] are marked (black points).

[Sparks et al., 1997; Mastin et al., 2009], and the power-law scaling is close to the one-quarter power expected from dimensional analysis. The pre-factor in (28) is determined from solutions of the integral model using the parameters given in Table 1 and the source conditions given in Table 3, and has a dependence on the source conditions, in particular the temperature contrast between the plume and the atmosphere. The influence of the model parameters and source conditions can be assessed by determining the power-law scaling (28) from model calculations in quiescent environments or, alternatively, by using an approximate scaling law relationship for the rise height of volcanic plumes in a quiescent atmosphere as a function of the model parameters and source conditions [see, e.g., Wilson et al., 1978; Settle, 1978; Woods, 1988; Sparks et al., 1997; Degruyter and Bonadonna, 2012] given by

$$H_0 \approx \frac{0.0013}{\sqrt{k_s}} \left(\frac{g \left(C_{p0} T_0 - C_a T_{a0} \right)}{\rho_{a0} C_a T_{a0}} \right)^{1/4} N^{-3/4} Q^{1/4}, \quad (29)$$

for H_0 measured in kilometer.

[31] Assuming that the shear rate of the atmospheric wind is constant in the troposphere, the shear rate can be written as $\dot{\gamma} = V_1/H_1$, where H_1 is the height of the tropopause and $V_1 = V(H_1)$ is the wind speed at the tropopause. A functional approximation for the height of rise (above the vent) of volcanic plumes in a constant shear wind field, which remain in the troposphere, with the wind speed explicitly included can be constructed by combining equation (27) with (28) to give

$$H = 0.318 Q^{0.253} \frac{1 + 1.373 \widetilde{\mathcal{W}}_s}{1 + 4.266 \widetilde{\mathcal{W}}_s + 0.3527 \widetilde{\mathcal{W}}_s^{\,2}}, \quad (30)$$

with $\widetilde{\mathcal{W}}_s = 1.44 V_1/(NH_1)$, where the dimensionless constant here is chosen by fitting to numerical solutions of the dry volcanic plume model with constant wind shear in a Standard Atmosphere. During the first explosive phase of the Eyjafjallajökull eruption, 14–17 April 2010, the wind parameter is estimated to take values in the range $0 < \widetilde{\mathcal{W}}_s < 1.1$ (Figure 4), where the wind speed at a height $H_1 = 7$ km has been taken as representative of the wind conditions. The approximation given in equation (30) well describes the rise heights calculated using the integral volcanic plume model for eruption columns which remain within the troposphere, at altitudes below 11 km (Figure 5). Above the tropopause, the wind field is modeled with a uniform wind speed and the atmospheric stratification in the Standard Atmosphere changes, and therefore, the simple approximation in equation (30) inevitably deviates from the model predictions.

[32] The semi-empirical relationship given by equation (30) is similar to the relationship between source mass flux and plume height in a wind field proposed by Degruyter and Bonadonna [2012]. However, whereas the relationship of Degruyter and Bonadonna [2012] is based on a linear combination of asymptotic results for plume rise in a quiescent atmosphere and for a plume which immediately bends over in a strong uniform wind field, the relationship (30) is obtained from a consideration of pure plumes rising in a linear shear crosswind in the intermediate regime where the plume rise speed and wind speed are comparable.

3. Integral Model of Moist Volcanic Eruption Columns in a Crosswind

[33] The addition of water vapor into the eruption column, either from entrainment of moist atmospheric air during the ascent of the plume or from the evaporation of surface water at the vent, can have a significant effect on the height of rise of the column [Woods, 1993; Koyaguchi and Woods, 1996; Sparks et al., 1997; Mastin, 2007]. Water vapor in the column at low altitude is transported to higher altitudes where the column may become saturated with respect to water vapor, and the water vapor will then condense to liquid water or ice, releasing latent heat to the column, increasing the column temperature, and promoting the rise of the plume. For phreatomagmatic eruptions, such as the first explosive phase of the 2010 Eyjafjallajökull eruption [Höskuldsson et al., 2011; Magnússon et al., 2012], there could be a significant incorporation of melt water into the eruption column at the source, decreasing the temperature of the plume at the source and increasing the gas content and moisture loading of the eruption column [Koyaguchi and Woods, 1996].

[34] The moisture content of an eruption column can be included in an integral model of volcanic plumes [Morton, 1957; Woods, 1993; Koyaguchi and Woods, 1996; Glaze et al., 1997; Mastin, 2007; Degruyter and Bonadonna, 2012] by accounting for phase changes of the water within the column and the effect of phase changes on the energy budget. Here we follow the formulation of Woods [1993] [see also Sparks et al., 1997]. In contrast, Degruyter and Bonadonna [2012] adopt the formulation of Glaze et al. [1997], which additionally includes an adiabatic cooling of the gaseous phases appropriate for vapor plumes. However, the equation for the conservation of heat flux presented by Degruyter and Bonadonna [2012] is obtained from the Glaze et al. [1997] conservation of energy equation assuming that the heat capacity of the atmosphere is independent of the moisture content of the atmosphere and the bulk density of the plume is equal to the atmospheric density. Note that we neglect phase change of water vapor and liquid water to ice. Although such phase transformations release latent heat to the column, the latent heat of freezing is about a factor of 10 smaller than the latent heat of vaporization [Sparks et al., 1997]. Therefore, the effect of moisture on the eruption column dynamics can be assessed, to leading order, by neglecting the complicated phase change to ice.

[35] We assume that the gas released at the vent is composed entirely of water vapor released from magma in the conduit and water vapor from the evaporation of ground water. Water vapor is entrained into the eruption column from the moist atmosphere and is advected with the bulk flow. Therefore, conservation of water in the column can be written as

$$\frac{\mathrm{d}}{\mathrm{d}s}(Q\phi) = 2\rho_a U_e R \phi_a, \quad (31)$$

where ϕ is the mass fraction of liquid water and water vapor in the column, and ϕ_a is the mass fraction of water vapor in the atmosphere (i.e., the specific humidity of the atmosphere).
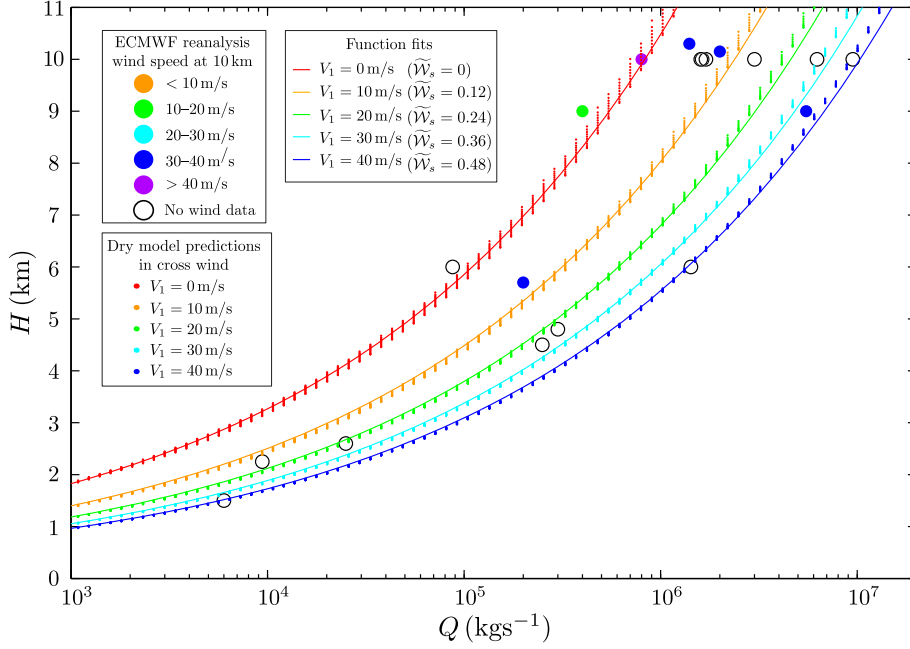
Figure 5. The rise height of an eruption column, H, as a function of the mass flux of material from the volcanic vent, Q, and wind speed at the tropopause, V_1. Predictions of the integral model of volcanic plumes in a crosswind that increases linearly with altitude up to a speed V_1 at the tropopause at an altitude of $H_1 = 11$ km are computed using the U.S. Standard Atmosphere [*COESA*, 1976] to describe the temperature profile in the atmosphere (with a buoyancy frequency $N = 0.0108 \, \text{s}^{-1}$), for a range of exit velocities and vent radii (the source conditions employed are given in Table 3). Functional approximations of the form $H = 0.318 Q^{0.253} \left(1 + 1.373\widetilde{\mathcal{W}}_s\right) / \left(1 + 4.266\widetilde{\mathcal{W}}_s + 0.3527\widetilde{\mathcal{W}}_s^2\right)$, where $\widetilde{\mathcal{W}}_s = 1.44 V_1/(NH_1)$, well describe the model predictions. The model predictions, and the function fits, are in good agreement with observations of rise height and mass flux from a dataset of historic eruptions [*Sparks et al.*, 1997; *Mastin et al.*, 2009], indicated by data points on the figure.

The mass fraction of water vapor in the column is denoted by ϕ_v, and $\phi_w = \phi - \phi_v$ is the mass fraction of liquid water in the plume.

[36] Condensation is assumed to occur rapidly once the eruption column has become saturated with respect to water vapor, such that the column remains saturated. Thus, once saturated, the mass fraction of gas in the column, which is composed of water vapor, denoted by w, remains at a value such that the partial pressure of water vapor, P_v, is equal to the saturation vapor pressure in the column, $e_s(T)$, so $P_v = e_s(T)$ [*Koyaguchi and Woods*, 1996]. We assume that no condensation occurs when the partial pressure of water vapor in the plume is less than the saturation vapor pressure. Note that $\phi_v = nw$ where n is the mass fraction of gas (dry air and water vapor) in the column. Assuming the gas phase is a mixture of water vapor and dry air, and each component can be considered an ideal gas, the partial pressure of water vapor is given by

$$P_v = w \frac{\rho_g}{\rho_v} P_a = \frac{wR_v}{wR_v + (1-w)R_a} P_a, \quad (32)$$

where ρ_g is the density of the gas phase, ρ_v is the density of water vapor, R_v and R_a are the specific gas constants of water vapor and dry air, respectively, and P_a is the pressure in the column which is assumed to adjust instantaneously to the local atmospheric pressure. Here we adopt a simple empirical

Table 4. Parameters Employed in the Moist Volcanic Plume Model

Parameter	Symbol	Value	Unit
Atmospheric pressure at sea level	P_{a0}	100	kPa
Atmospheric temperature at sea level	T_{a0}	293	K
Density of liquid water	ρ_w	1000	kg m^{-3}
Density of solid pyroclasts	ρ_s	1200	kg m^{-3}
Entrainment coefficient in absence of wind	k_s	0.09	
Entrainment coefficient due to wind	k_w	0.9	
Gas constant of dry air	R_a	285	$\text{J K}^{-1}\text{kg}^{-1}$
Gas constant of water vapor	R_v	462	$\text{J K}^{-1}\text{kg}^{-1}$
Gravitational acceleration	g	9.81	m s^{-2}
Height of stratosphere	H_2	20	km
Height of tropopause	H_1	11	km
Lapse rate of temperature in stratosphere	λ	2.0	K km^{-1}
Lapse rate of temperature in troposphere	μ	6.5	K km^{-1}
Latent heat of vaporization at 273 K	L_{c0}	2.5×10^6	J kg^{-1}
Parameter in saturation vapor pressure relation	a_1	2.53×10^{11}	Pa
Parameter in saturation vapor pressure relation	a_2	5.42×10^3	K
Specific heat capacity of dry air	C_a	998	$\text{J K}^{-1}\text{kg}^{-1}$
Specific heat capacity of liquid water	C_w	4200	$\text{J K}^{-1}\text{kg}^{-1}$
Specific heat capacity of solid pyroclasts	C_s	1617	$\text{J K}^{-1}\text{kg}^{-1}$
Specific heat capacity of water vapor	C_v	1850	$\text{J K}^{-1}\text{kg}^{-1}$

approximation for the saturation vapor pressure [*Rogers and Yau*, 1989; *Woods*, 1993],

$$e_s(T) = a_1 \exp(-a_2/T), \quad (33)$$

for dimensional constants a_1 and a_2 given in Table 4 and temperature, T, measured in kelvin. More sophisticated approximations to solutions of the Clausius-Clapeyron equation could be employed in the integral model.

[37] The enthalpy of the mixture of dry air, water vapor, liquid water, and solid pyroclasts is given by

$$h = (n - \phi_v)C_a T + \phi_s C_s T + \phi_v C_v T + \phi_w h_w, \quad (34)$$

where $\phi_s = 1 - n - \phi_w$ is the mass fraction of solids and C_a, C_s, and C_v are the specific heat capacities at constant pressure of dry air, solid pyroclasts, and water vapor, respectively. The enthalpy of liquid water condensed from the water vapor in the column, h_w, is related to the enthalpy of the water vapor through

$$h_w = C_v T - L_c(T), \quad (35)$$

where $L_c(T)$ is the latent heat of vaporization at temperature T. Assuming that the specific heat capacities are independent of temperature, the latent heat of vaporization can be approximated as $L_c(T) = L_{c0} + (C_v - C_w)(T - T_0)$ [*Gill*, 1982], where L_{c0} is the latent heat of vaporization at $T_0 = 273$ K and the specific heat capacities of water vapor and liquid water at constant pressure, C_v and C_w, respectively, are measured in $J\,K^{-1}\,kg^{-1}$. Therefore, the enthalpy of the mixture can be written as follows:

$$h = (n - \phi_v)C_a T + \phi_s C_s T + \phi_v C_v T + \phi_w C_w T - \phi_w L_c(T_0). \quad (36)$$

[38] The equation for conservation of total energy, accounting for the release of latent heat on condensation of water vapor in a saturated eruption column, becomes

$$\frac{d}{ds}\left(\rho U R^2 \left(C_p T + \frac{U^2}{2} + gz\right)\right)$$
$$= 2\rho_a R U_e \left(C_A T_a + \frac{U_e^2}{2} + gz\right) \quad (37)$$
$$+ L_{c0} \frac{d}{ds}\left(\rho R^2 U(\phi - \phi_v)\right),$$

where C_p is the bulk specific heat capacity at constant pressure of the column, given by

$$C_p = nC_g + \phi_w C_w + (1 - n - \phi_w)C_s, \quad (38)$$

$C_g = wC_v + (1 - w)C_a$ is the specific heat capacity at constant pressure of the gas phase, and C_A is the specific heat capacity at constant pressure of the moist atmosphere.

[39] The bulk density of the column is determined by equating the specific volume of the column with the partial volumes of the water vapor, dry air, liquid water, and solid pyroclasts:

$$\frac{1}{\rho} = \frac{n}{\rho_g} + \frac{\phi_w}{\rho_w} + \frac{1 - n - \phi_w}{\rho_s}, \quad (39)$$

where ρ_w is the density of liquid water (assumed constant in the atmosphere). The density of the gas phase is given by

$$\rho_g = \frac{P_a}{R_g T}, \quad (40)$$

where the bulk gas constant of the column is given by

$$R_g = wR_v + (1 - w)R_a. \quad (41)$$

[40] Neglecting the fallout of solid pyroclasts during the ascent of the material in the column, conservation of the solid phase can be used to determine the variation of the gas mass fraction,

$$n = 1 - \phi_w - (1 - n_0)\frac{Q_0}{Q}. \quad (42)$$

[41] The moisture content of the atmosphere is characterized by the relative humidity of the atmosphere, denoted by R_H, which is defined [*WMO*, 1988] as the ratio of the vapor pressure in the atmosphere to the saturation vapor pressure of the atmosphere, given by $e_s(T_a)$. The moisture content of the atmosphere, ϕ_a, is related to the relative humidity by

$$\phi_a = \frac{R_H e_s(T_a) R_a}{R_v P_a - R_H e_s(T_a)(R_v - R_a)}. \quad (43)$$

[42] The specific heat capacity of the moist atmosphere is given by

$$C_A = \phi_a C_v + (1 - \phi_a)C_a, \quad (44)$$

where we have assumed that all water in the atmosphere is in vapor form. Equations (32), (33), and (38)–(44) complete the closures for the thermodynamics in the moist plume model.

[43] In a quiescent environment, the release of latent heat upon condensation can significantly enhance the height to which a volcanic plume ascends [*Woods*, 1993; *Sparks et al.*, 1997; *Mastin*, 2007]. The largest influence of the phase change of water occurs for small or moderately sized eruptions (with source mass flux $Q_0 < 10^6$ kg s^{-1}), where the energy released on condensation contributes significantly to the energy of the plume [*Sparks et al.*, 1997] (Figure 6). For larger eruptions that ascend into the stratosphere, the contribution from latent heat of condensation has less effect on the rise of the plume [*Woods*, 1993] (Figure 6) since the latent heat released on condensation of water vapor is significantly less than the heat content of the erupted material [*Woods*, 1993; *Sparks et al.*, 1997]. A similar enhancement of the rise of volcanic plumes due to latent heating is found for plume rising in a crosswind, as shown in Figure 6 where predictions for the rise heights of dry volcanic plumes, where there is no phase change of water and the atmosphere is dry, are compared to those obtained with the moist plume model where water vapor condenses during the ascent of the plume through a moist atmosphere. In order to assess the maximum effect of the moisture content of the plume and atmosphere, the atmosphere is assumed to have relative humidity $R_H = 1$ throughout. We note that for this
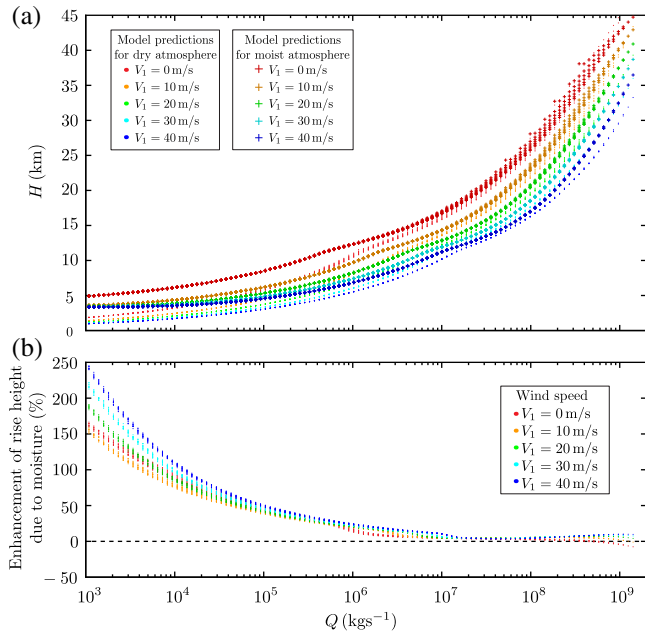
Figure 6. The rise height of an eruption column, H, as a function of the mass flux of material from the volcanic vent, Q, for dry and moist atmospheres. (a) Predictions of the integral model of dry volcanic plumes in a crosswind are compared with predictions from the integral model of moist volcanic plumes in a crosswind. A range of exit velocities and vent radii are used, with the source conditions employed given in Table 3. (b) The enhancement of the rise height of moist volcanic plumes in comparison to dry volcanic plumes as a function of the mass flux of material from the volcanic vent. The crosswind increases linearly with altitude up to the tropopause (at an altitude of 11 km) and is constant above. The atmospheric temperature is described using the U.S. Standard Atmosphere [*COESA*, 1976]. For the moist plume model, the atmosphere is assumed to have the maximum vapor loading, with a relative humidity $R_H = 1$ throughout the atmosphere. The parameter values used in the moist plume model are given in Table 4.

high moisture loading, the ambient atmosphere is convectively unstable [*Gill*, 1982] up to an altitude of approximately 4 km. This results in a weak dependence of the rise height on wind speed and mass flux for small eruptions (with mass flux $Q < 10^4$ kg s^{-1}) which reach altitudes of around 3.5 km (Figure 6a) and consequently a large enhancement of the rise height of moist plumes in a wind field over similar plumes in a dry atmosphere (Figure 6b). For lower atmospheric vapor loadings, the enhancement of the plume rise height due to phase change of water is reduced.

## 4. The Wind-blown Plume at Eyjafjallajökull 2010

[44] We have shown that an integral model of volcanic plumes in a Standard Atmosphere and a shear wind field can be used to calibrate a relationship between rise height and mass flux, given by equation (30), which explicitly includes the wind speed through the parameter $\widetilde{\mathcal{W}}_s$.

However, the ascent of the eruption column is also affected by the local atmospheric conditions [*Sparks et al.*, 1997], which may not be captured when the atmosphere is described by a Standard Atmosphere. For example, varying atmospheric stratification and altitudes of the troposphere-tropopause and tropopause-stratosphere boundaries between tropical, mid-latitude, and polar regions can result in large variation in the rise heights of volcanic plumes with equal source mass flux [*Woods*, 1995]. Furthermore, the atmospheric stratification above a volcano can change due to local weather systems and varies over the course of a day as the heat content of the atmosphere changes. Changing atmospheric stratification has been suggested as a cause of diurnal variations in the rise height of weak plumes during the effusive phase, 19–24 April 2010, at Eyjafjallajökull [*Petersen et al.*, 2012]. In addition, the linear shear wind profile adopted above may not be a sufficiently detailed description of the atmospheric winds to reproduce accurately the observed plume rise heights. Instead, by employing observational data of the atmosphere, with measured profiles of the wind speed, temperature, pressure, and relative humidity, the integral model can be used to assess the effects of the local atmospheric conditions.

[45] By varying source conditions in the integral model, the rise height predicted by the model can reproduce approximately the plume height observed at Eyjafjallajökull at 1200 UTC on 14 April. The resulting source conditions are given in Table 5. Solutions of the integral model using atmospheric data representing the changing meteorological conditions during the first explosive phase of the Eyjafjallajökull eruption, 14–17 April 2010, are shown in Figure 7 with source conditions held fixed at the values given in Table 5. As the local meteorology at Eyjafjallajökull is not recorded, we employ radiosonde measurements of atmospheric conditions (wind speed, temperature, pressure, and relative humidity) which are made every 12 h at Keflavik International Airport (data obtained from Wyoming Weather Web [*Oolman*, 2012] repository of radiosonde soundings). Although Keflavik is 155 km from Eyjafjallajökull, the wind speeds measured by radiosondes are likely to be representative of the wind conditions at Eyjafjallajökull. Indeed, wind speeds predicted every 3 h by the U.K. Met Office Unified Model numerical weather prediction (NWP) scheme (NWP meteorological data provided by the U.K. Met Office from the Unified Model global data archive) and interpolated to approximate wind speeds above Eyjafjallajökull show similar wind speeds as those recorded by radiosondes (Figure 8a). Increased wind speeds on 15 and 16 April, compared to those observed on 14 April, result in enhanced bending over of the

Table 5. Source Conditions Employed to Approximately Reproduce Observed Height of the Plume From Eyjafjallajökull at 1200 UTC on 14 April 2010

Variable	Symbol	Value	Unit
Column temperature	T_0	1000	K
Exit angle	θ_0	0	
Exit velocity	U_0	60	m s^{-1}
Gas mass fraction	n_0	0.03	
Vent altitude	z_0	1666	m
Vent radius	R_0	80	m
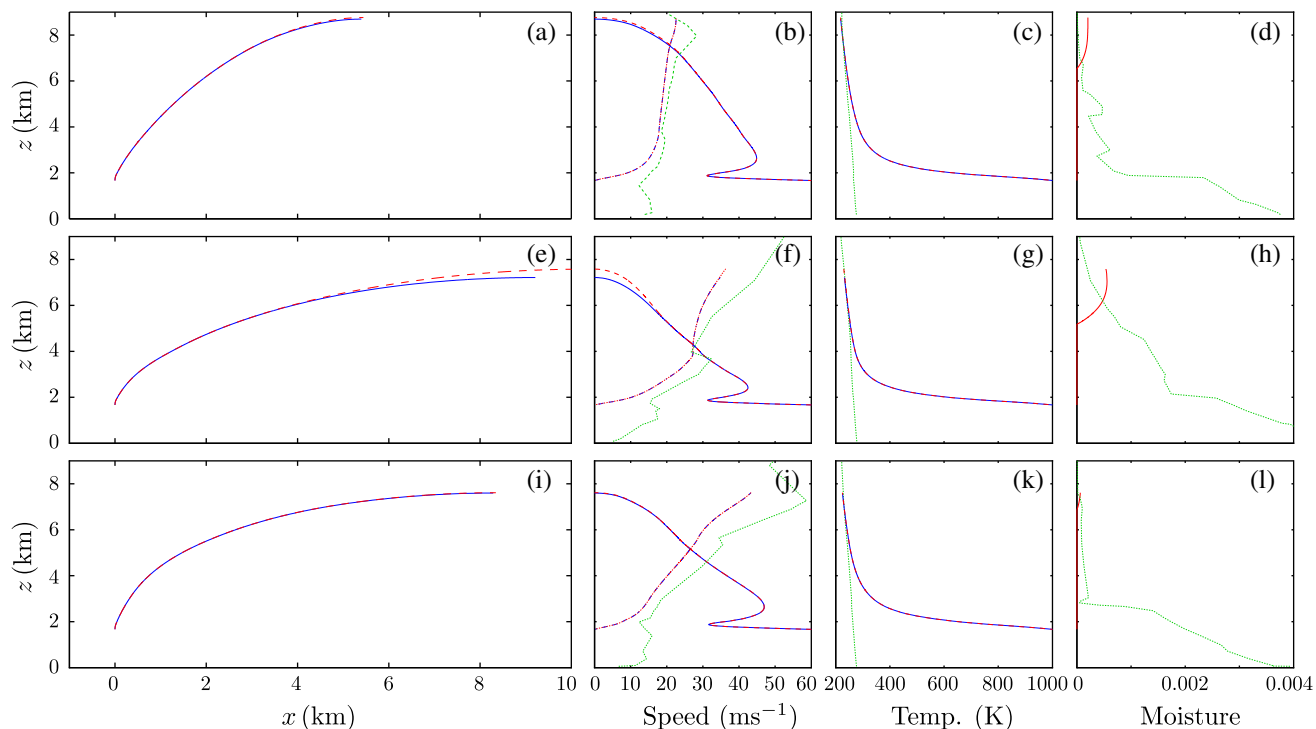
Figure 7. Solutions of the dry and moist wind-blown plume models with atmospheric conditions measured by radiosondes at Keflavik International Airport. Atmospheric conditions measured at (a–d) 1200 UTC on 14 April 2010, (e–h) 1200 UTC on 15 April 2010, and (i–l) 1200 UTC on 16 April 2010. Source conditions for the models are given in Table 5. Blue curves show solutions to the dry wind-blown plume model, red curves are solutions of the wet wind-blown plume model, and green curves show atmospheric conditions, linearly interpolated between data points. (a), (e), (i) Plume centerline trajectories. (b), (f), (j) Vertical plume speed (blue solid and red dashed lines), horizontal plume speed (blue dashed and red dotted lines), and horizontal atmospheric wind speed (green dashed line). (c), (g), (k) Temperature of the plume (blue solid and red dashed lines) and temperature of the atmosphere (green dashed line). (d), (h), (l) Mass fraction of liquid water in the plume (red solid line) and moisture content of the atmosphere (green dashed line).

plume trajectory and a reduction in the height of rise of the plume. The atmospheric temperature profiles on each day are similar, with atmospheric lapse rates of temperature (determined using linear least squares regression of observed temperatures up to an altitude of 9 km above sea level) of $\Gamma = 6.359$ K/km ($r^2 = 0.9950$) on 14 April, $\Gamma = 6.172$ K/km ($r^2 = 0.9886$) on 15 April, and $\Gamma = 6.373$ K/km ($r^2 = 0.9972$) on 16 April. Weak temperature inversions are observed on 14 and 16 April but have little effect on the plume motion.

[46] A comparison of solutions obtained from the moist and dry plume models with radiosonde measurements of atmospheric data is also shown in Figure 7. The model solutions coincide until water vapor begins to condense in the plume. The release of latent heat on condensation provides energy to the eruption column which can result in an enhancement of the rise height of the plume. However, condensed water is substantially more dense than water vapor, and so the phase change can reduce the rise height of the plume. The overall effect on the plume depends on the extent to which condensation occurs and therefore on the atmospheric vapor loading. For example, the moist plume model predicts the condensation of water vapor for the 14 April (Figure 7a–d), but the rise height of the plume is

almost identical to the prediction of a plume rising in a dry atmosphere. In contrast, the condensation predicted to occur by the moist plume model using atmospheric data from 15 April (Figure 7e–h) results in an increase in the rise height with respect to the dry plume model of approximately 367 m, a 5% enhancement in the rise height over a dry plume model. This difference is within the uncertainty of the rise heights observed during the Eyjafjallajökull 2010 eruption (Figure 8); so for small wind-affected volcanic eruptions, the role of external moisture added to an eruption column is secondary to the role of atmospheric stratification, source buoyancy flux, and wind.

[47] During the 2010 Eyjafjallajökull eruption, a weather radar at Keflavik International Airport, 155 km west of Eyjafjallajökull, measured plume heights above the summit of the volcano at 5-min intervals [*Arason et al.*, 2011; *Petersen et al.*, 2012], providing a record of the changing plume heights over the course of the eruption. The scanning strategy utilized by the weather radar [*Arason et al.*, 2011] and the distance from Keflavik to Eyjafjallajökull result in semi-discrete jumps in the observed plume heights [*Arason et al.*, 2011], and measured plume heights are lower bounds on the actual rise height of the eruption column. In order to

reduce the spurious jumps in the radar record of plume heights, we therefore take maximum observed heights in 1-h intervals. Furthermore, the heights recorded in the radar dataset are measured heights above the summit of Eyjafjal-lajökull, while the plume may not have reached the maximum altitude until some distance downwind [*Arason et al.*, 2011]. Despite these limitations, the radar time series of plume heights represents the most complete record of plume height variation during the Eyjafjallajökull eruption.

[48] The plume height observed during the first explosive phase of the Eyjafjallajökull eruption, 14–17 April 2010, varied on a 24-h time scale [*Petersen*, 2010; *Arason et al.*, 2011], with the plume reaching an altitude in excess of 8 km on 14 April ($\widetilde{\mathcal{W}}_s \approx 0.43$), falling to 5–7 km on 15 April ($\widetilde{\mathcal{W}}_s \approx 0.95$ at 0000 UTC; $\widetilde{\mathcal{W}}_s \approx 0.80$ at 1200) and on 16 April ($\widetilde{\mathcal{W}}_s \approx 1.10$ at 0000; $\widetilde{\mathcal{W}}_s \approx 1.01$ at 1200), and rising again to over 8 km on 17 April ($\widetilde{\mathcal{W}}_s \approx 0.23$ at 0000; $\widetilde{\mathcal{W}}_s \approx 0.57$ at 1200) (Figures 4 and 8b, and 8c). The plume height variations are coincident with meteorological changes, and in particular, plume heights are anti-correlated with wind speeds, as shown in Figure 8.
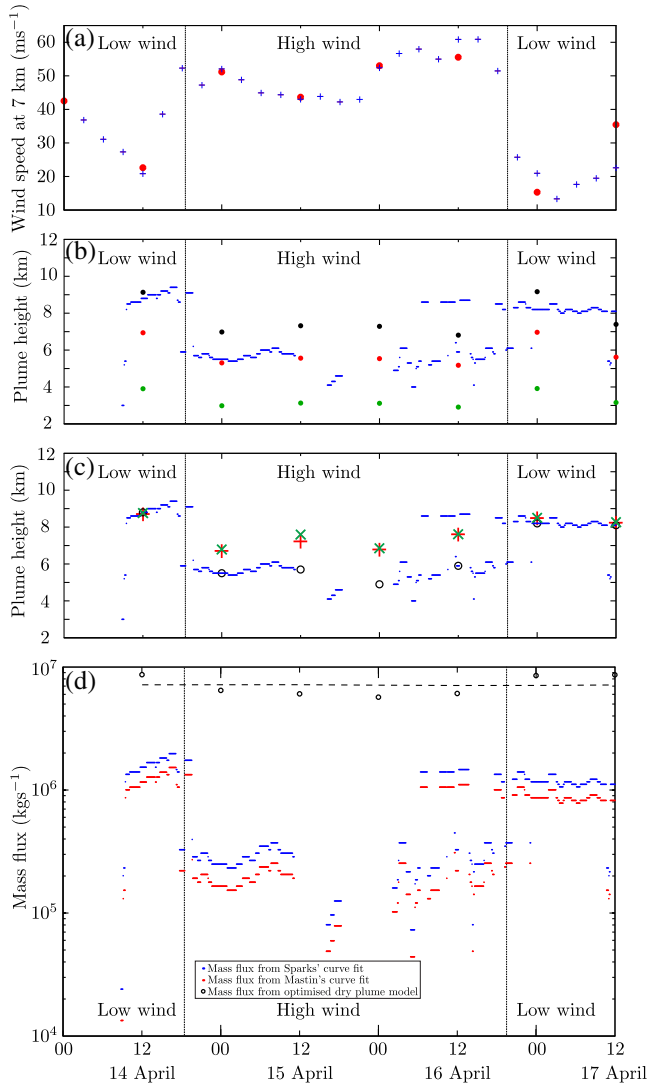
[49] The mass flux of material from Eyjafjallajökull can be estimated by using equations (27) and (29), with appropriate estimates of source conditions and with the wind strength parameter $\widetilde{\mathcal{W}}_s$ determined from radiosonde measurements of the atmospheric wind. The wind speed V_1 is taken as the speed recorded at $H_1 = 7$ km as the wind profiles show an approximately linearly increasing wind speed up to this altitude over the course of the first explosive phase. In Figure 8b, we show the plume rise height predicted by equations (27) and (29) with source conditions given in Table 5 and the source mass flux held constant. The variation in the predicted plume rise height in Figure 8b is therefore due to the changing wind conditions over the duration of the first explosive phase. Figure 8b shows that the variation in the observed plume height can be described by the semi-empirical relationship when a constant source mass flux of $Q = 6 \times 10^6$ kg s^{-1} is assumed. In contrast, a source mass flux of $Q = 2 \times 10^6$ kg s^{-1} (chosen to represent the peak source mass flux predicted by the *Sparks et al.* [1997] and *Mastin et al.* [2009] relationships for the rise heights observed at Eyjafjallajökull) underpredicts the rise height during periods of low wind speeds, and a source mass flux of $Q = 2 \times 10^5$ kg s^{-1} (chosen to represent the minimum source mass flux predicted by the *Sparks et al.* [1997] and *Mastin et al.* [2009] curve fits) underpredicts the observed rise height.

[50] The semi-empirical relationship given by equation (30) is unable to fully capture the variations in observed plume heights as the detailed atmospheric conditions are

Figure 8. Comparison of the wind-blown plume models to observations of plume rise heights at Eyjafjallajökull during the first explosive phase, 14–17 April 2010. (a) Wind speed at an altitude of 7 km (taken as characteristic of the wind conditions) as a function of time during 14–17 April 2010. Wind speeds measured every 12 hours by radiosondes at Keflavik International Airport (red circles) and predicted every three hours by the U.K. Met Office Unified Model (blue +). (b) Plume rise heights at Eyjafjallajökull, recored by a weather radar at Keflavik (blue ·), and predictions of rise heights from the semi-empirical relationship between source mass flux and plume rise height as functions of time. The mass flux is fixed at $Q = 6 \times 10^6$ kgs^{-1} (black circles), $Q = 2 \times 10^6$ kgs^{-1} (red circles) and $Q = 2 \times 10^5$ kgs^{-1} (green circles). (c) Plume rise heights at Eyjafjallajökull, recored by a weather radar at Keflavik (blue ·), and predictions of rise heights from the wind-blown dry (red +) and moist (green ×) plume models as functions of time. In addition, predictions from the dry model with optimized source conditions (black ○) reproduce precisely observed plume rise heights. (d) Source mass flux estimate as a function of time. When estimated from the observed plume heights using curve fits to a dataset of historic eruptions [*Sparks et al.*, 1997; *Mastin et al.*, 2009] the mass flux of material from the source varies over more than an order of magnitude, whereas the mass flux in the wind-blown plume model remains approximately constant (dashed line). Optimized model solutions can be found with source conditions varied to reproduce exactly observed plume rise heights (Table 6), with source mass flux constrained to be within 25% of the source mass flux adopted in the non-optimized calculations.

Table 6. Optimized Source Conditions Employed to Reproduce Observed Height of the Plume from Eyjafjallajökull, 14–17 April 2010

Time	Exit Velocity U_0 (m s^{-1})	Column Temperature T_0 (K)	Gas Mass Fraction n_0	Mass Flux Q (kg s^{-1})
14 April 1200	76.5	925.7	0.034	8.729×10^6
15 April 0000	96.1	766.2	0.070	6.502×10^6
15 April 1200	99.9	784.3	0.076	6.090×10^6
16 April 0000	50.0	600.0	0.052	5.722×10^6
16 April 1200	94.5	637.0	0.086	6.136×10^6
17 April 0000	83.0	821.7	0.042	8.581×10^6
17 April 1200	83.6	861.6	0.040	8.695×10^6

not included. However, detailed meteorological observations can be employed in the integral models of volcanic plumes. In Figure 8c, plume rise height predictions are obtained from the dry and moist integral models. Source conditions are chosen to reproduce approximately the observed plume height at 1200 UTC on 14 April (Table 5) and subsequently held fixed while the meteorology varies. The changing atmospheric conditions, in particular the wind speed, in the integral models can account for observed variations in the rise height of the plume from Eyjafjallajökull during 14–17 April 2010 (Figure 8b). However, in order to reproduce precisely the observed plume heights, an adjustment of the source conditions is required. Optimized solutions of the dry plume model are obtained by varying the exit velocity of material at the vent, the column temperature at the vent, and the mass fraction of gas in the column at the vent (Table 6). Given the nonlinear dependence of the plume rise height on these source conditions, the set of source conditions which reproduce the observed rise height may not be unique, and here we have not attempted to explore systematically the solution space of the optimized solutions.

[51] If the changing meteorological conditions are not considered, the changes in plume rise heights during this period suggest that the source mass flux, determined from curve fits to the dataset of historic eruptions [*Sparks et al.*, 1997; *Mastin et al.*, 2009], varies by more than an order of magnitude and often by two orders of magnitude (Figure 8d). However, solutions of the wind-blown plume model which employ contemporaneous meteorological data obtained from radiosondes are able to reproduce the observed variation in plume rise height with a near constant source mass flux (Figure 8d). Furthermore, the optimized solutions of the dry plume model precisely reproduce observed plume height variations (Figure 8c) with the source mass flux varying in the range 5.722×10^6–8.729×10^6 kg s^{-1}. As there is no independent evidence for large changes in the source mass flux during the first explosive phase of the 2010 Eyjafjallajökull eruption on the time scale of the observed variation in plume height, the changing meteorology during the course of the eruption must be explicitly included in models or expression used to relate source mass flux to plume height.

5. Discussion

[52] In order to forecast accurately the concentration of ash in the atmosphere during volcanic crises, source conditions describing the transport of material from the volcano to the atmosphere, in particular the height at which ash starts to intrude horizontally and the mass flux of material released from the volcano, are required. In a quiescent atmosphere, a scaling relationship between source mass flux and plume rise height can be used to estimate the source mass flux during an eruption [*Sparks et al.*, 1997; *Mastin et al.*, 2009]. Calibrations of the scaling relationships have not considered atmospheric controls on the ascent of volcanic plumes yet have been used in situations where meteorology has strongly affected plume behavior [*Webster et al.*, 2012].

[53] Atmospheric winds have a crucial influence on the injection of volcanic ash into the atmosphere and must be accounted for when estimating source mass flux. In windy environments, the additional entrainment of ambient air into the plume, together with the bending over of the plume trajectory, significantly reduces the rise height of the plume relative to an equivalent source in a quiescent environment. Thus, to attain equal rise heights, a plume in a strong wind field has a significantly higher source mass flux than a plume in a quiescent atmosphere.

[54] If detailed measurements of local atmospheric conditions are available, the meteorological data can be incorporated into integral models of volcanic plumes in a crosswind. The source conditions of the model can then be varied in an attempt to reproduce observed plume heights and provide an estimate of the source mass flux. In the absence of detailed meteorological observations, new semi-empirical relationships between plume height and source mass flux which explicitly include the wind speed, through the wind shear rate, provide improved estimates of the source mass flux for weak, bent-over plumes.

[55] The record of plume rise heights at Eyjafjallajökull during the first explosive phase of the 2010 eruption shows abrupt changes in the plume height [*Arason et al.*, 2011; *Petersen et al.*, 2012]. One explanation, based on the use of calibrated relationships between plume height and source mass flux, is that the source strength of Eyjafjallajökull varied by more than an order of magnitude during this time period. However, there is no independent evidence of such large, abrupt changes in the source mass flux during the first explosive phase of the eruption. Our results show that an alternative explanation is that the source mass flux varied little during the first explosive phase and that changes in plume heights are predominantly due to meteorological changes, in particular changes in the atmospheric wind speed. Sudden changes in plume height are better explained by rapid changes in wind speed than large changes in the volcanic source mass flux by more than an order of magnitude that are coincident with meteorological changes.

[56] Our results highlight that the source mass flux deduced from observations of plume height, which is input into far-field atmospheric ash dispersion models, can be significantly underestimated unless the effects of wind on the near-source plume dynamics are considered. This has important consequences on the predictions of ash concentrations in the far field. The ash concentration levels for commercial flight operations adopted in Europe during the 2010 Eyjafjallajökull eruption increase the demand on atmospheric dispersion forecasts. In order to distinguish 'safe' airspace from 'no-fly' zones [*ICAO*, 2010; *CAA*, 2011], the dispersion models must predict ash

concentrations to within $1\,\mathrm{mg\,m^{-3}}$. While improved observations near the source and in the far field, together with advances in the numerical dispersion models, can assist in achieving accurate forecasts of ash concentration, the source condition input into the models remains a crucial component. An increase in the source mass flux by an order of magnitude could result in the prediction of large regions of airspace being closed to traffic as 'safe' ash concentrations in the atmosphere are exceeded. Therefore, underpredictions of the source mass flux by an order of magnitude or more due to the neglect of wind on the plume rise could limit the ability of ash dispersion models to forecast ash concentrations and manage airspace during volcanic crises.

6. Conclusions

[57] Integral models of volcanic plumes in a wind field allow the relationship between the rise height of volcanic plumes, source conditions at the volcanic vent, and atmospheric conditions to be explored. Detailed meteorological descriptions from atmospheric soundings or numerical weather prediction forecasts can be employed in the integral models, and source conditions varied to reproduce observed rise heights of volcanic plumes, providing estimates of volcanic source conditions. When atmospheric profiles are not available, a new semi-empirical relationship between plume rise height and source mass flux that explicitly includes the atmospheric wind speed can provide improved estimates of source mass flux over existing calibrated scaling relationships. Our results demonstrate that the source mass flux determined from plume rise height can be significantly underestimated unless the effect of atmospheric wind is considered [*Briggs*, 1969; *Hewett et al.*, 1971; *Bursik*, 2001; *Degruyter and Bonadonna*, 2012], and variations in plume rise height can be attributed to changing meteorology rather than large changes in source mass flux.

Appendix A: Pure Plume Model in a Linear Shear Cross Flow

[58] Simple estimates of the effect of the crosswind on the rise of volcanic plumes can be found by examining a pure plume model for which the multiphase character of volcanic plumes is not considered and a simple atmosphere with uniform stable stratification is assumed. While the volcanic plume model has several controlling parameters, the pure plume model contains only two controlling dimensionless parameters, and therefore, the influence of the controlling parameters on the character of solutions to the pure plume model can be determined readily.

[59] The integral model of a pure plume in a crosswind [*Hewett et al.*, 1971] can be obtained from the wind-blown volcanic plume model by assuming that (i) the material in the column is a gas with the same specific heat capacity and gas constant as the atmosphere, and both of these quantities remain constant; (ii) the thermal energy of the column greatly exceeds the kinetic energy; (iii) the fluids in the plume and atmosphere are incompressible (so mass conservation can be replaced by volume conservation); and (iv) the density difference between the plume and the ambient atmosphere is small in comparison with a reference density, so

the Boussinesq approximation can be invoked. Defining the volume flux, πq, specific momentum flux, πm, and specific buoyancy flux, πf, as

$$q = R^2 U, \quad m = R^2 U^2, \quad f = R^2 U g', \tag{A1}$$

where $g' = g(\rho_a - \rho)/\rho_{a0}$ is the reduced gravity, with ρ_{a0} a reference density of the atmosphere; the equations governing the steady plume dynamics [*Hewett et al.*, 1971] are

$$
\begin{aligned}
\frac{\mathrm{d}q}{\mathrm{d}s} &= \frac{2q}{\sqrt{m}} U_e, \\
\frac{\mathrm{d}m}{\mathrm{d}s} &= V\cos\theta\frac{\mathrm{d}q}{\mathrm{d}s} + \frac{qf}{m}\sin\theta, \\
m\frac{\mathrm{d}\theta}{\mathrm{d}s} &= -V\sin\theta\frac{\mathrm{d}q}{\mathrm{d}s} + \frac{qf}{m}\cos\theta, \\
\frac{\mathrm{d}f}{\mathrm{d}s} &= -N^2 q\sin\theta, \\
\frac{\mathrm{d}x}{\mathrm{d}s} &= \cos\theta, \\
\frac{\mathrm{d}z}{\mathrm{d}s} &= \sin\theta.
\end{aligned}
\tag{A2}
$$

Here the buoyancy frequency, N, is given by

$$N^2 = -\frac{g}{\rho_{a0}}\frac{\mathrm{d}\rho_a}{\mathrm{d}z}. \tag{A3}$$

[60] Solutions of the governing equations are sought for a pure plume ($f(0) = f_0 > 0$, $q(0) = 0$, $m(0) = 0$) from a point source at $x = z = 0$ in a linearly stratified ambient (N^2 constant).

[61] Dimensionless governing equations can be formed by introducing dimensionless variables (denoted with hats) by scaling the dimensional variables using the source buoyancy flux f_0 and buoyancy frequency N,

$$
\begin{aligned}
s &= k_s^{1/2} f_0^{1/4} N^{-3/4}\hat{s}, & x &= k_s^{-1/2} f_0^{1/4} N^{-3/4}\hat{x}, \\
z &= k_s^{-1/2} f_0^{1/4} N^{-3/4}\hat{z}, & f(s) &= f_0\hat{f}(\hat{s}), \\
q(s) &= k_s^{1/2} f_0^{3/4} N^{-5/4}\hat{q}(\hat{s}), & m(s) &= f_0 N^{-1}\hat{m}(\hat{s}).
\end{aligned}
\tag{A4}
$$

We note the scalings introduced anticipate that the rise height of the plume scales with the buoyancy flux to the one-quarter power [*Morton et al.*, 1956] when the ambient is quiescent ($V = 0$). The dimensionless governing equations become

$$\frac{\mathrm{d}\hat{q}}{\mathrm{d}\hat{s}} = \frac{2\hat{q}}{\sqrt{\hat{m}}}\left(\left|\frac{\hat{m}}{\hat{q}} - \mathcal{W}\cos\theta\right| + \kappa|\mathcal{W}\sin\theta|\right), \tag{A5}$$
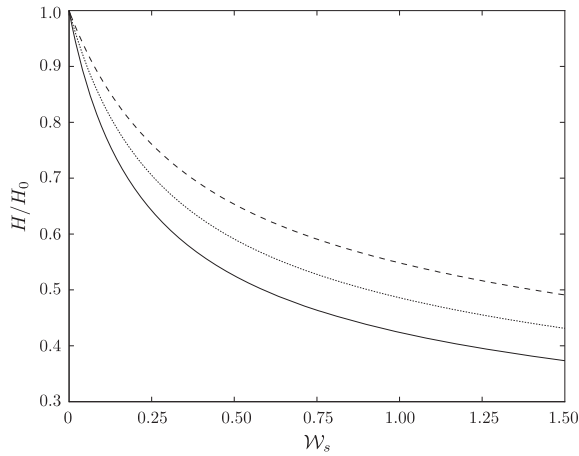
$$\frac{\mathrm{d}\hat{m}}{\mathrm{d}\hat{s}} = \frac{\hat{f}\hat{q}}{\hat{m}}\sin\theta + \mathcal{W}\cos\theta\frac{\mathrm{d}\hat{q}}{\mathrm{d}\hat{s}}, \tag{A6}$$

$$\hat{m}\frac{\mathrm{d}\theta}{\mathrm{d}\hat{s}} = \frac{\hat{f}\hat{q}}{\hat{m}}\cos\theta - \mathcal{W}\sin\theta\frac{\mathrm{d}\hat{q}}{\mathrm{d}\hat{s}}, \tag{A7}$$

$$\frac{\mathrm{d}\hat{f}}{\mathrm{d}\hat{s}} = -\hat{q}\sin\theta, \tag{A8}$$

$$\frac{\mathrm{d}\hat{x}}{\mathrm{d}\hat{s}} = \cos\theta, \tag{A9}$$

$$\frac{\mathrm{d}\hat{z}}{\mathrm{d}\hat{s}} = \sin\theta. \tag{A10}$$

Figure A1. The height of neutral buoyancy for pure plumes in a linear shear flow as a function of the wind strength parameter $\mathcal{W}_s$ and the ratio of the entrainment coefficients κ with $\kappa = 10$ (solid line), $\kappa = 7$ (dotted line), and $\kappa = 5$ (dashed line). The height of neutral buoyancy, H, is normalized by the height of neutral buoyancy for a pure plume in a quiescent environment, H_0. The ambient environment is uniformly stably stratified.

[62] The dimensionless equations depend on two dimensionless parameters, the ratio of the entrainment coefficients $\kappa = k_w/k_s$, and the ratio of the wind speed to the typical buoyancy-driven rise speed of the plume

$$\mathcal{W} = \frac{\sqrt{k_s}V}{f_0^{1/4}N^{1/4}}. \qquad (A11)$$

[63] For volcanic eruption columns, the buoyancy flux at the source can be related to the mass flux [*Sparks et al.*, 1997] through

$$f_0 = g\left(\frac{C_pT - C_aT_a}{C_aT_a}\right)\frac{Q}{\rho_{a0}}, \qquad (A12)$$

from which we obtain equation (25).

[64] If the cross wind is taken as a linear shear flow with shear rate $\dot{\gamma}$, so $V(z) = \dot{\gamma}z$, we find

$$\mathcal{W} = \frac{\dot{\gamma}}{N}\hat{z} = \mathcal{W}_s\hat{z}, \qquad (A13)$$

where $\mathcal{W}_s = \dot{\gamma}/N$. Experimental observations [*Hewett et al.*, 1971] suggest $\kappa = 10$, and we adopt this value here.

[65] Solutions to the system of dimensionless governing equations (A5)–(A10) for varying crosswind speeds can be computed numerically by varying the parameter $\mathcal{W}_s$, allowing the effect of the wind speed on the rise height to be determined. In addition, the influence of the relative magnitude of the entrainment coefficients can be investigated by varying κ. In a linear shear flow, the computations show that H/H_0 monotonically decreases with $\mathcal{W}_s$ (Figures 4 and A1), where H_0 is the rise height of a plume in a quiescent environment. A rational function of the form

$$\frac{H}{H_0} = \frac{1 + a\mathcal{W}_s}{1 + b\mathcal{W}_s + c\mathcal{W}_s^2} \qquad (A14)$$

can be used to approximate the curves in Figure A1, with the fitting coefficients being functions of κ. The functional relationship between the rise height and the wind parameter $\mathcal{W}_s$ is well approximated by the rational function given in equation (27) in the range $\mathcal{W}_s < 5$, for $\kappa = 10$. For $5 \leq \kappa \leq 10$, the linear relationships $a = 0.87 + 0.50\kappa$, $b = 1.09 + 0.32\kappa$, and $c = 0.06 + 0.03\kappa$ can be used to estimate the fitting coefficients in equation (A14).

References

Arason, P., G. N. Petersen, and H. Bjornsson (2011), Observations of the altitude of the volcanic plume during the eruption of Eyjafjallajökull, April–May 2010, *Earth Sys. Sci. Data*, 3(1), 9–17, doi:10.5194/essd-3-9-2011.

Barsotti, S., A. Neri, and J. S. Scire (2008), The VOL-CALPUFF model for atmospheric ash dispersal: 1. Approach and physical formulation, *J. Geophys. Res.*, 113, B03208, doi:10.1029/2006JB004623.

Bonadonna, B., A. Folch, S. Loughlin, and H. Puempel (2012), Future developments in modelling and monitoring of volcanic ash clouds: Outcomes from the first IAVCEI-WMO workshop on Ash Dispersal Forecast and Civil Aviation, *B. Volcanol.*, 74(1), 1–10, doi:10.1007/s00445-011-0508-6.

Bonadonna, C., R. Genco, M. Gouhier, M. Pistolesi, R. Cioni, F. Alfano, A. Hoskuldsson, and M. Ripepe (2011), Tephra sedimentation during the 2010 Eyjafjallajökull eruption (Iceland) from deposit, radar, and satellite observations, *J. Geophys. Res.*, 116, B12202, doi:10.1029/2011JB008462.

Briggs, G. A. (1969), Optimum formulas for buoyant plume rise, *Philos. Trans. R. Soc. London*, 265, 197–203, doi:10.1098/rsta.1969.0048.

Bursik, M. (2001), Effect of wind on the rise height of volcanic plumes, *Geophys. Res. Lett.*, 28(18), 3621–3624, doi:10.1029/2001GL013393.

Bursik, M. I., S. E. Kobs, A. Burns, O. A. Braitseva, L. I. Bazanova, I. V. Melekestsev, A. Kurbatov, and D. C. Pieri (2009), Volcanic plumes and wind: Jetstream interaction examples and implications for air traffic, *J. Volcanol. Geotherm. Res.*, 186(1–2), 60–67, doi:10.1016/j.jvolgeores.2009.01.021.

CAA (2011), Guidance regarding flight operations in the vicinity of volcanic ash (Version 2), *Technical Notice*, Civil Aviation Authority.

Carazzo, G., E. Kaminski, and S. Tait (2006), The route to self-similarity in turbulent jets and plumes, *J. Fluid Mech.*, 547, 137–148, doi:10.1017/S002211200500683X.

COESA (1976), U.S. Standard Atmosphere, NOAA.

Degruyter, W., and C. Bonadonna (2012), Improving on mass flow rate estimates of volcanic eruptions, *Geophys. Res. Lett.*, 39, L16308, doi:10.1029/2012GL052566.

Dellino, P., M. T. Gudmundsson, G. Larsen, D. Mele, J. A. Stevenson, T. Thordarson, and B. Zimanowski (2012), Ash from the Eyjafjallajökull eruption (Iceland): Fragmentation processes and aerodynamic behavior, *J. Geophys. Res.*, 117, B00C04, doi:10.1029/2011JB008726.

Ernst, G. G. J., R. S. J. Sparks, S. N. Carey, and M. I. Bursik (1996), Sedimentation from turbulent jets and plumes, *J. Geophys. Res.*, 101(B3), 5575–5589, doi:10.1029/95JB01900.

Gill, A. E. (1982), Atmosphere—Ocean Dynamics, International Geophysics Series, Academic Press, London.

Glaze, L. S., and S. M. Baloga (1996), Sensitivity of buoyant plume heights to ambient atmospheric conditions: Implications for volcanic eruption columns, *J. Geophys. Res.*, 101(D1), 1529–1540, doi:10.1029/95JD03071.

Glaze, L. S., S. M. Baloga, and L. Wilson (1997), Transport of atmospheric water vapor by volcanic eruption columns, *J. Geophys. Res.*, 102(D5), 6099–6108, doi:10.1029/96JD03125.

Gudmundsson, M. T., A. Hoskuldsson, G. Larsen, T. Thordarson, B. Oddsson, T. Hognadottir, I. Jonsdottir, H. Bjornsson, N. G. Petersen, and E. Magnusson (2011), Eyjafjallajökull April–June 2010: An explosive-mixed eruption of unusually long duration, *Geophys. Res. Abstr.*, 13, EGU2011–12,542.

Hewett, T. A., J. A. Fay, and D. P. Hoult (1971), Laboratory experiments of smokestack plumes in a stable atmosphere, *Atmos. Environ.*, 5(9), 767–789, doi:10.1016/0004-6981(71)90028-X.

Höskuldsson, Á., et al. (2011), Eruption dynamics of the 2010 summit eruption at the Eyjafjallajökull volcano (Iceland): Magma fragmentation, tephra stratigraphy and transport, *Geophys. Res. Abstr.*, 13, EGU2011–14,165.

ICAO (2010), Volcanic Ash Contingency Plan—Eur and Nat Regions, *EUR Doc 019—NAT Doc 006, Part II*, International Civil Aviation Authority.

Kaminski, E., S. Tait, and G. Carazzo (2005), Turbulent entrainment in jets with arbitrary buoyancy, *J. Fluid Mech.*, 526, 361–376, doi:10.1017/S0022112004003209.

Kaye, N. B. (2008), Turbulent plumes in stratified environments: A review of recent work, *Atmos. Ocean*, 46(4), 433–441, doi:10.3137/ao.460404.

Koyaguchi, T., and A. W. Woods (1996), On the formation of eruption columns following explosive mixing of magma and surface-water, *J. Geophys. Res.*, 101(B3), 5561–5574, doi:10.1029/95JB01687.

Langmann, B., A. Folch, M. Hensch, and V. Matthias (2012), Volcanic ash over Europe during the eruption of Eyjafjallajökull on Iceland, April–May 2010, *Atmos. Environ.*, 48, 1–8, doi:10.1016/j.atmosenv.2011.03.054.

Magnússon, E., M. Gudmundsson, M. Roberts, G. Sigurðsson, F. Höskuldsson, and B. Oddsson (2012), Ice-volcano interactions during the 2010 Eyjafjallajökull eruption, as revealed by airborne imaging radar, *J. Geophys. Res.*, 117, B07405, doi:10.1029/2012JB009250.

Mastin, L. G. (2007), A user-friendly one-dimensional model for wet volcanic plumes, *Geochem. Geophys. Geosyst.*, 8(3), Q03014, doi:10.1029/2006GC001455.

Mastin, L. G., et al. (2009), A multidisciplinary effort to assign realistic source parameters to models of volcanic ash-cloud transport and dispersion during eruptions, *J. Volcanol. Geotherm. Res.*, 186(1–2), 10–21, doi:10.1016/j.jvolgeores.2009.01.008.

Morton, B. R. (1957), Buoyant plumes in a moist atmosphere, *J. Fluid Mech.*, 2, 127–144, doi:10.1017/S0022112057000038.

Morton, B. R., G. Taylor, and J. S. Turner (1956), Turbulent gravitational convection from maintained and instantaneous sources, *Philos. Trans. R. Soc. London A. Mat.*, 234(1196), 1–23, doi:10.1098/rspa.1956.0011.

Newhall, C. G., and S. Self (1982), The volcanic explosivity index (VEI): An estimate of explosive magnitude for historical volcanism, *J. Geophys. Res.*, 87(C2), 1231–1238, doi:10.1029/JC087iC02p01231.

Oolman, L. (2012), Wyoming Weather Web, http://weather.uwyo.edu.

Petersen, G. N., H. Bjornsson, and P. Arason (2012), The impact of the atmosphere on the Eyjafjallajökull 2010 eruption plume, *J. Geophys. Res.*, 117, D00U07, doi:10.1029/2011JD016762.

Petersen, G. N. (2010), A short meteorological overview of the Eyjafjallajökull eruption 14 April–23 May 2010, *Weather*, 65(8), 203–207, doi:10.1002/wea.634.

Rogers, R., and M. Yau (1989), A Short Course in Cloud Physics, third ed., Pergamon Press, Oxford.

Scase, M. M. (2009), Evolution of volcanic eruption columns, *J. Geophys. Res.*, 114, F04003, doi:10.1029/2009JF001300.

Self, S. (2006), The effects and consequences of very large explosive volcanic eruptions, *Philos. Trans. R. Soc. A*, 364(1845), 2073–2097, doi:10.1098/rsta.2006.1814.

Settle, M. (1978), Volcanic eruption clouds and the thermal power output of explosive eruptions, *J. Volcanol. Geotherm. Res.*, 3, 309–324, doi:10.1016/0377-0273(78)90041-0.

Siebert, L., and T. Simkin (2002–2012), Volcanoes of the world: An illustrated catalog of holocene volcanoes and their eruptions. Smithsonian Institution, Global Volcanism Program Digital Information Series GVP-3, http://www.volcano.si.edu/world/.

Sparks, R. S. J. (1986), The dimensions and dynamics of volcanic eruption columns, *B. Volcanol.*, 48(1), 3–15, doi:10.1007/BF01073509.

Sparks, R. S. J., M. I. Bursik, S. N. Carey, J. S. Gilbert, L. S. Glaze, H. Sigurdsson, and A. W. Woods (1997), Volcanic Plumes, John Wiley & Sons, Chichester, U.K.

Stevenson, J. A., et al. (2012), Distal deposition of tephra from the Eyjafjallajökull 2010 summit eruption, *J. Geophys. Res.*, 117, B00C10, doi:10.1029/2011JB008904.

Webster, H. N., et al. (2012), Operational prediction of ash concentrations in the distal volcanic cloud from the 2010 Eyjafjallajökull eruption, *J. Geophys. Res.*, 117, D00U08, doi:10.1029/2011JD016790.

Wilson, L., R. S. J. Sparks, T. C. Huang, and N. D. Watkins (1978), The control of volcanic column heights by eruption energetics and dynamics, *J. Geophys. Res.*, 83(B4), 1829–1836, doi:10.1029/JB083iB04p01829.

WMO (1988), General meteorological standards and recommended practices, *Technical Regulations No. 49 Vol. 1*, World Meteorological Organization.

Woods, A. W. (1988), The fluid dynamics and thermodynamics of eruption columns, *B. Volcanol.*, 50(3), 169–193, doi:10.1007/BF01079681.

Woods, A. W. (1993), Moist convection and the injection of volcanic ash into the atmosphere, *J. Geophys. Res.*, 98(B10), 17,627–17,636, doi:10.1029/93JB00718.

Woods, A. W. (1995), The dynamics of explosive volcanic eruptions, *Rev. Geophys.*, 33(4), 495–530, doi:10.1029/95RG02096.

Woods, A. W. (2010), Turbulent plumes in nature, *Annu. Rev. Fluid Mech.*, 42, 391–412, doi:10.1146/annurev-fluid-121108-145430.

Woods, A. W., and M. I. Bursik (1991), Particle fallout, thermal disequilibrium and volcanic plumes, *B. Volcanol.*, 53, 559–570, doi:10.1007/BF00298156.